5-6-2014

Synthesis of Pyrrole-modified Porphyrins: Oxachlorins, and the Beckmann Rearrangement of Octaethyl-2-oxa-chlorin Oxime

Eileen V. Meehan
Emeehan311@gmail.com

Synthesis of Pyrrole-modified Porphyrins: Oxachlorins, and the Beckmann Rearrangement of Octaethyl-2-oxa-chlorin Oxime

Eileen Meehan

B.S., The University of Connecticut, 2012

A Thesis

Submitted in Partial Fulfillment of the

Requirement for the Degree of

Master of Science

at the

University of Connecticut

2014

APPROVAL PAGE

Master of Science Thesis

Synthesis of Pyrrole-modified Porphyrins: Oxachlorins, and the Beckmann Rearrangement of Octaethyl-2-oxa-chlorin Oxime

Presented by

Eileen Meehan

Major Advisor:

_____

Dr. Christian Brückner

Associate Advisor:

_____

Dr. Edward Neth

Associate Advisor:

_____

Dr. James Bobbitt

Associate Advisor:

_____

Dr. Michael Smith

University of Connecticut

2014

Table of Contents

List of Abbreviations

aq	aqueous
^{13}C NMR	^{13}C nuclear magnetic resonance
conc	concentrated
d	doublet
ESI	electrospray ionization
^{1}H NMR	^{1}H nuclear magnetic resonance
Hz	Hertz
λ	wavelength
m	multiplet
MS	mass spectrometry
ν	frequency
r.t.	room temperature
s	singlet
t	triplet
TLC	thin layer chromatography
UV-vis	ultraviolet-visible

List of Instruments

UV-Visible spectroscopy	VARIAN CARY 50
Fluorescence spectroscopy	VARIAN CARY ECLIPSE
NMR spectroscopy	BRUKER AVANCE 300
	BRUKER AVANCE III 400
	BRUKER AVANCE 500
HR-MS	AB SCIEX Q-STAR-ELITE
	JEOL ACCUTOF LC-PLUS
LR-MS	WATERS QUATTRO II
IR-spectroscopy	THERMO NICOLET NEXUS 670
	BRUKER ALPHA

List of Publications

This thesis is in part based on the following in print and planned publications:

- Ogikubo, J.; Meehan, E.; Engle, J. T.; Ziegler, C. J.; Brückner, C. *meso*-Aryl-3-alkyl-2-oxachlorins *J. Org. Chem*. **2012**, *77(14)*, 6199–6207.

- Meehan, E.; Li, R.; Zeller, M.; Brückner, C. 'The Beckmann Rearrangement of a β-Octaalkyl-β-oxochlorin Oxime' in preparation.

- Meehan, E.; Brückner, C. 'β-Heptaalkyloxazolochlorin: The Back to the Future Porphyrin' in preparation.

Other current and planned publications with EM co-authorship:

- Ogikubo, J.; Meehan, E.; Engle, J. T.; Ziegler, C. J.; Brückner, C. *meso*-Tetraphenyl-2-oxabacteriochlorins and *meso*-Tetraphenyl-2, 12/13-dioxabacteriochlorins. *J. Org. Chem*. **2013**, *78(7)*, 2840–2852.

- Graefe, S.; Ogikubo, J.; Meehan, E.; Brückner, C.; Wiehe, A. 'Evaluation of the *in cyto* PDT Efficacy of Oxazolo-chlorins and -bacteriochlorins', in preparation for *J. Photochem. Photobiol.*

List of Figures

List of Schemes

List of Tables

Acknowledgements

First, I would like to start by saying thank you, Dr. Neth, for inspiring me to join a lab. Dr. Brückner, thank you for letting me join your lab, and then letting me stick around! Thank you for letting me bother you (almost all the time), and for your patience, and time with Mia!

To past Brückner group members: thank you for all of your advice. Junichi (J), thank you for taking me on as your undergrad and guiding and mentoring me. Jill, thank you for making lab a warm and welcoming place and making my experience in lab a positive one. Lalith, your positivity helped keep me going—thank you for the constant smiles!

To current group members: thank you all for putting up with my craziness, all the loud laughter and what I would like to call my "loud indoor talking voice". Ruoshi, I appreciate all of the support you have given me this semester—thank you. Mike L., thank you for being someone I could always count on. Meenakshi, I will miss our trips to the grocery store! Sarina, thank you for listening to me! Nisansala, I am so sorry you got stuck with the desk behind me! Steven (Hubbers/Blimps/Stavros)- you helped get me through this last semester and kept me smiling; thank you for letting me bother you all.the.time. And remember, you're pretty.

Mike (Bffl/BFFR)- thank you so much for constantly offering your support, lending an ear and putting up with me. Chris (Cristov)- thank you for always letting me take up your time and going out of your way for me.

Mommy- I am sorry for all the grey hairs I have caused. There isn't just one thing I can thank you for, though—I am so grateful for you. Tierney (Wuffles), I am glad you lived right around the corner for me to bother! Tony (Buddy!), yes, yes, it all started back in elementary school with intestine man—thank you for inspiring me to stick with Science. And, Bert<3.

1. Introduction to Porphyrins and Chlorins

1.1 Porphyrins, Chlorins, and Bacteriochlorins

Porphyrins are a family of intensely colored, fully unsaturated aromatic macrocycles.[1,2] They are comprised of four pyrrolic subunits which are linked by four methine bridges; these methylene carbons are labeled the *meso*-positions, while the peripheral pyrrolic positions are referred to as the β-positions (Figure 1-1).[2]

Porphyrins contain 22 conjugated π electrons but only 18 π electrons are necessary to maintain a closed conjugated aromatic system. The remaining 4 π electrons located at two β,β'-double bonds, are cross-conjugated with the aromatic system, allowing the prophyrin macrocycle to be described as an 18+4 π Hückel aromat.[3] Since the cross-conjugated double bonds are not part of the central aromatic system, they can be removed from conjugation. The removal of the cross-conjugated double bonds significantly alters the chemical and physical properties of the resulting chromophores from those of the parent porphyrin.

The reduction of a single β,β'-double bond, leading to the formation of a pyrroline subunit, results in the formation of a chlorin chromophore.[1,2] The reduction of two β,β'-double bonds, on opposing pyrrolic units of the macrocycle, results in the formation of a bacteriochlorin.[1,2] However, reducing the β,β'-double bonds on adjacent pyrroles results in the formation of a bacteriochlorin isomer, an isobacteriochlorin.[1] The closed conjugated aromatic 18 π system of these hydroporphyrin macrocycles still remains intact.

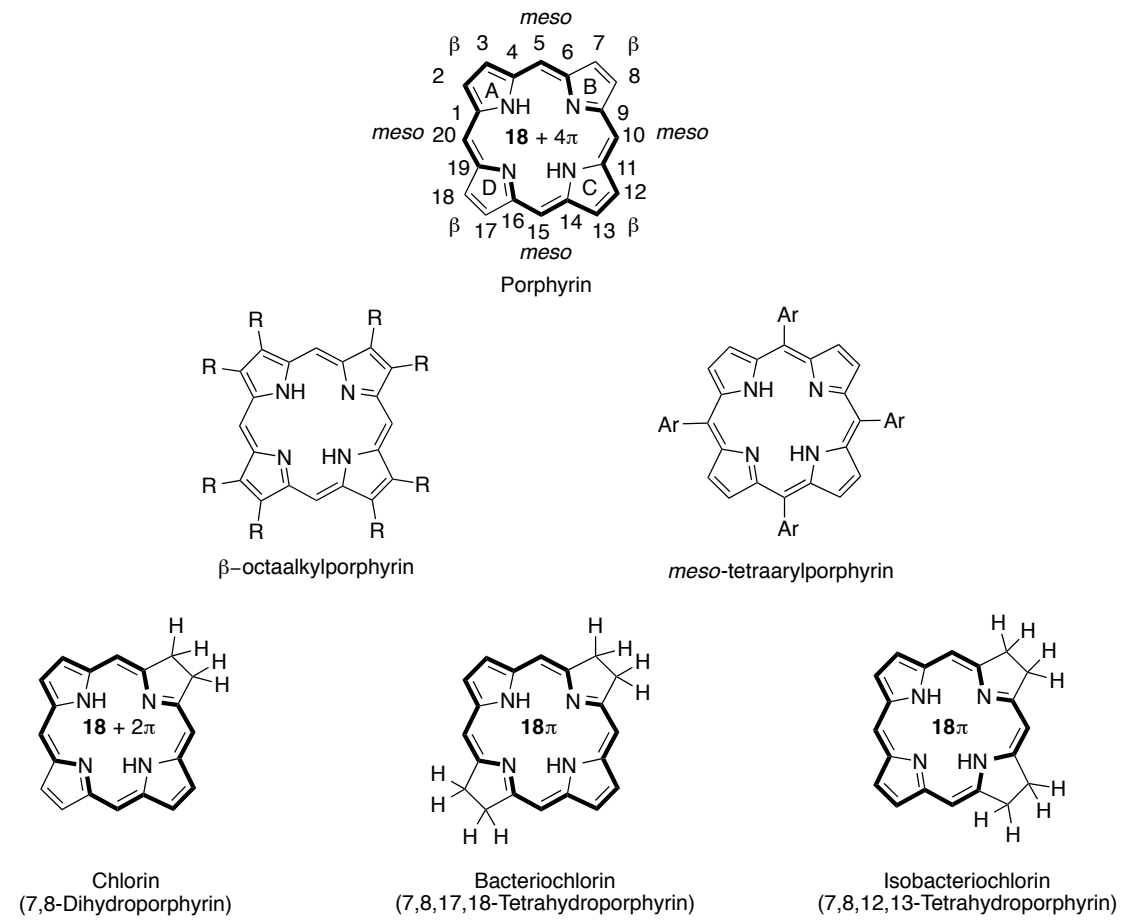

Figure 1-1. Structure, position numbering, and the naming system used for porphyrins and hydroporphyrins. Bold regions indicate the 18 π–aromatic system.

Since porphyrins can undergo reactions typical of aromatic compounds, a variety of chemical transformations have been employed for the conversion of porphyrins. In addition, the 'pseudo-olefinic' nature of the β,β'-double bonds allows for the application of reactions characteristic of olefins.

The photophysical and chemical properties of porphyrins and hydroporphyrins are a reflection of the presence of their conjugated π-systems. Modification to the porphyrin macrocycle alters the UV-visible spectra in a diagnostic fashion (more detailed discussion presented in Section 1.5).

1.2 Naturally Occurring Porphyrins, Chlorins, and Bacteriochlorins

Porphyrins, chlorins, and bacteriochlorins are ubiquitous in nature. They are involved in a variety of biological processes and can be found in plants and blood.[3] For example, the iron complex of protoporphyrin IX, heme, is a prosthetic group with critical roles in vertebrate and invertebrate organisms (Figure 1-2).[4] Heme is found in hemoglobin, myoglobin and cytochromes with involvement in oxygen transport and storage, and electron transfer.[2,4]

Examples of naturally occurring chlorins include chlorophyll *a* which are responsible for the green color of leaves. The magnesium chlorin complex acts as a light harvesting pigment and is essential for photosynthesis in all plants.[2,4] In fact, they are essential for all higher life forms. Moreover, the bacteriochlorin magnesium complex, bacteriochlorophyll *a*, is the photosynthetic pigment that is found in photoautotrophic purple bacteria and cyanobacteria (Figure 1-2).[4]

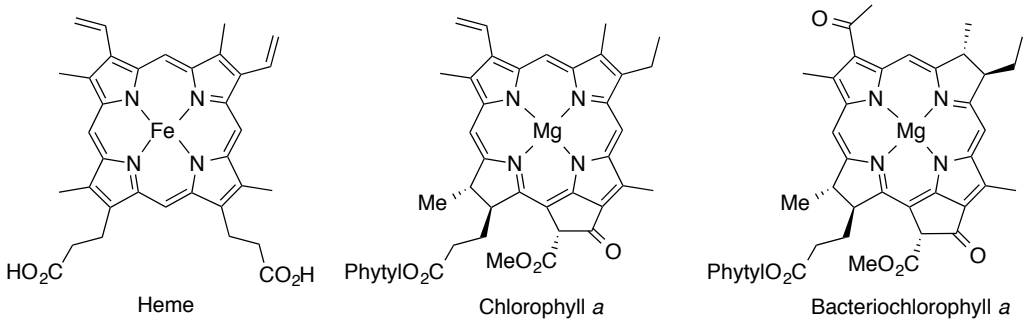

Figure 1-2. Examples of a naturally occurring porphyrin, chlorin and bacteriochlorin.

1.3 Synthesis of Porphyrins and Chlorins

While it is possible to isolate and purify the naturally occurring β-octaalkylated porphyrins, the methods to extract and isolate these porphyrins involve arduous multi-step procedures, and many are not stable outside their natural protein environments. As an alternative to extracting porphyrins from their natural resources, methods to synthesize naturally occurring

and synthetic porphyrins, such as *meso*-aryl porphyrins, of which do not have any known natural counterparts, have been employed.

1.3.1 *meso*-Tetraarylporphyrins

meso-Aryl porphyrins are a simple to synthesize, synthetic class of porphyrins (Scheme 1-1). *meso*-Substituted porphyrin synthesis is achieved via a 1 × 4 condensation, in which four monopyrrolic units join to form a porphyrin. The condensation of aryl aldehydes and pyrrole will form *meso*-tetraarylporphyrins in up to 30% yield in crystalline form in a single step.

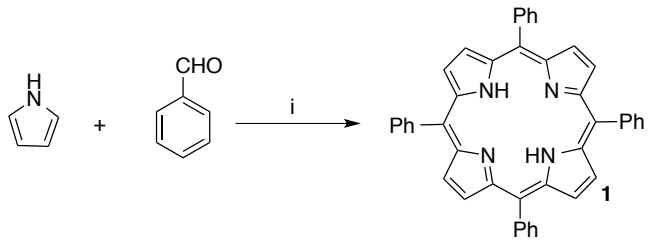

Scheme 1-1. Adler/Longo synthesis of *meso*-tetraphenylporphyrin.
Reaction Conditions: i. propionic acid, reflux, air.

In 1936, Rothemund developed a one-step, one-pot approach to the synthesis of *meso*-tetraarylporphyrins.[5] He achieved this via the direct condensation of benzaldehyde and a pyrrole in pyridine in sealed tubes at high temperatures.[5] The harsh conditions of this reaction resulted in poor yields, and was later modified resulting in scalable conditions and improved yield (~20-30% yield) by Adler and Longo in the 1960's (Scheme 1-1).[6]

The mechanism of the Adler and co-worker acid-catalyzed tetraarylporphyrin synthesis has been elucidated (Scheme 1-2)[1]. This acid-catalyzed electrophilic aromatic substitution (EAS) reaction between a pyrrole and a benzaldehyde forms an intermediate carbinol **2**.[1] Acid treatment generates a resonance-stabilized cation from **2**, which then undergoes a second EAS with another pyrrole to form 5-phenyldipyrromethane **3**.[1] This sequence repeats until a ring closing

condensation of tri-phenyltetrapyrromethane **5** with benzaldehyde occurs to form a tetrapyrrolic porphyrinogen **6**.[1] The formation of the fully unsaturated aromatic porphyrin, *meso*-tetraphenylporphyrin **7** occurs via the *in situ* oxidation of **6**.[1] Generally, compound **1** will crystallize out of the solution and can be isolated via filtration.

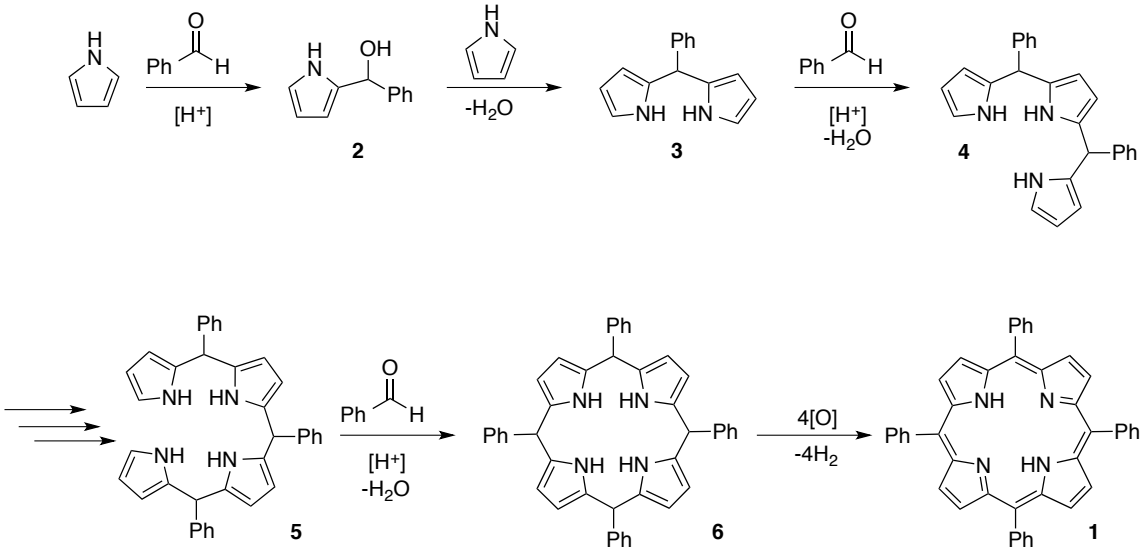

Scheme 1-2. Mechanistic interpretation of the Adler synthesis of **1**.

Further, in the 1980's, Lindsey and coworkers developed and optimized a method for the synthesis of *meso*-tetraarylporphyrins.[7] However, Lindsey's higher yielding (~60% yield) 4 × 4 condensation method is only suitable for small scale syntheses, due to its requirement for highly diluted conditions.[7, 8] Comparatively, Adler's tetraarylporphyrin synthesis, although low in absolute yield (~20%), is advantageous in that it is a straightforward synthesis that requires no chromatography for purification, and can be scaled up to ~25 grams per reaction.

1.3.2 Synthesis of Chlorins

Unfortunately, unlike the synthesis of *meso*-tetraarylporphyrins, the synthesis of these porphyrin derivatives is not as facile. The pathways to chlorins (and bacteriochlorins) include:

extraction from natural resources, semi-synthetic approaches, total synthesis, as well as, pyrrole modified approaches (the modification of synthetic porphyrins).[10] Each approach offers distinct advantages and disadvantages.

In the late 1960's, Whitlock *et al*. described the reduction of TPP **1** by diimide (NH=NH), a reagent that is generated *in situ* by heating tosyl hydrazide with base, to produce dihydrochlorin **7** and tetrahydrobacteriochlorin **8** (Scheme 1-3).[11] The diimide reduction of TPP is a regioselective β,β'-double bond reduction. Unfortunately, it is limited by the difficulty of isolating the reaction products, as the hydroporphyrin is susceptible to oxidation back to the corresponding porphyrin **1**.

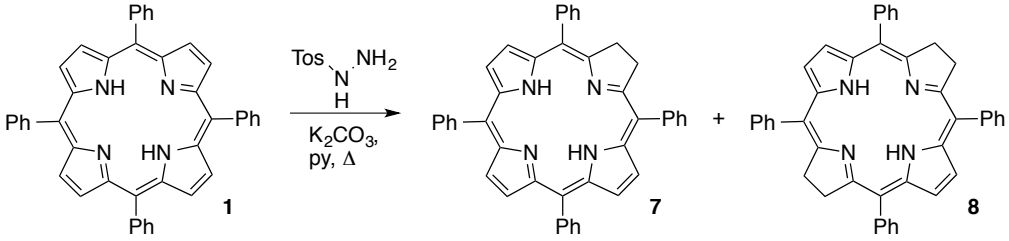

Scheme 1-3. Regioselective β,β'-double bond reduction of **1**.

In the 1940's, Fischer capitalized on the pseudo-olefinic nature of the β,β'-double bonds of the porphyrin macrocycle and reported the osmium tetroxide-mediated dihydroxylation of the β,β'-double bonds of octaalkylporphyrins.[12] This reaction was widely adopted and produced chlorins, bacteriochlorins, as well as, isobacteriochlorins.[13-24] Compared to the rapid reaction of a true olefin with osmium tetroxide, the dihydroxylation of porphyrins is slow, requiring several days.

In the 1990's, Brückner *et al.* applied the osmium tetroxide-mediated dihydroxylation to *meso*-tetraarylporphyrins.[3, 25-28] This highly region-selective reaction uses a stoichiometric amount (or stoichiometric excess) of OsO_4 in a solution of pyridine, which acts as a co-solvent

and accelerator, to produce a chlorin diol.[29-31] The intermediate osmate ester is then cleaved using H_2S to produce *meso*-tetraaryldihydroxychlorin **9** and *meso*-tetraaryltetrahydroxy-bacteriochlorin **10** (Scheme 1-4). [29-31] Unlike the diimide reduction, the diolchlorins and tetrahydroxybacteriochlorins produced are stable and resistant towards oxidation back towards the porphyrin. Interestingly, the reaction of metalloporhyrins generates regiospecifically isobacteriochlorins.

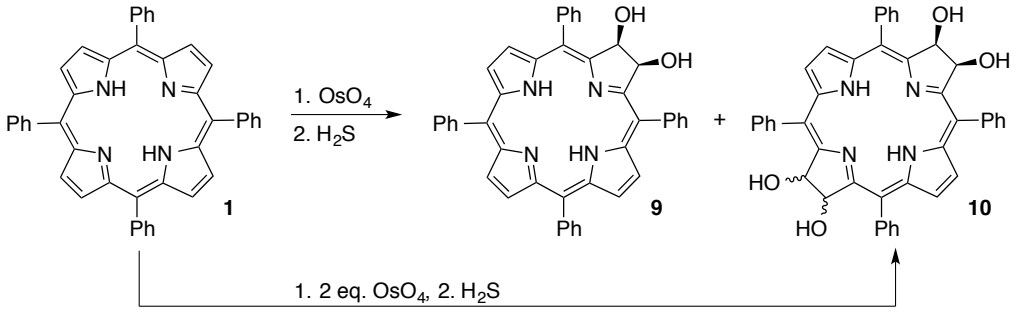

Scheme 1-4. Osmium tetroxide-mediated dihydroxylation of **1**.

In early 2000, Lindsey and co-workers presented refinement of a method previously pioneered by Woodward, Eschenmoser, and Battersby regarding the [2+2] synthesis of chlorins.[32, 33] These publications describe the synthesis of chlorins via the fusion of a dipyrromethane with a *gem*-dimethyldihydrodipyrrin (Scheme 1-5).[34-39] Most importantly, the presence of a *gem*-dimethyl moiety at the pyrrolidine β-position stabilizes the chlorin by acting as an inherent oxidation-protection. The total synthesis approach to synthesize chlorins allows for access to asymmetric chlorins without the need for the reduction of a β,β'-double bond. It also provides the ability to prepare chlorins with unsubsituted β- and *meso*-positions.

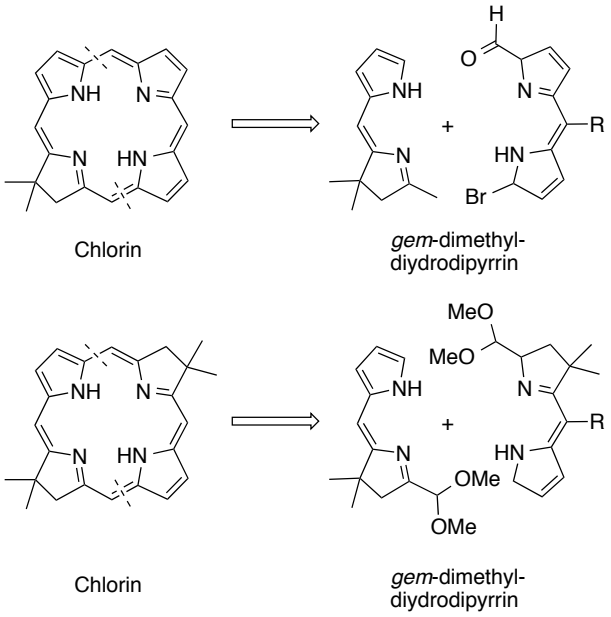

Scheme 1-5. Generalized scheme of the retrosynthetic analyses for the total syntheses of chlorins and bacteriochlorins along a [2+2] strategy.

1.4 Pyrrole-Modified Chlorins

When at least one pyrrolic subunit is formally replaced by a non-pyrrolic heterocycle, the resultant species is referred to as a pyrrole-modified porphyrin. These porphyrinoids can be made via step-wise conversion of a porphyrin or via total synthesis.

In the 1984, the oxidation of the porphyrin at the β-pyrrolic position of the porphyrin chromophore to form a pyrrole-modified porphyrin, was reported by Crossley and King.[40] The oxidation resulted in the presence of oxygen at the β-pyrrolic position of the porphyrin, forming *meso*-tetraphenylporpholactone (TPL) **13** (Scheme 1-6).

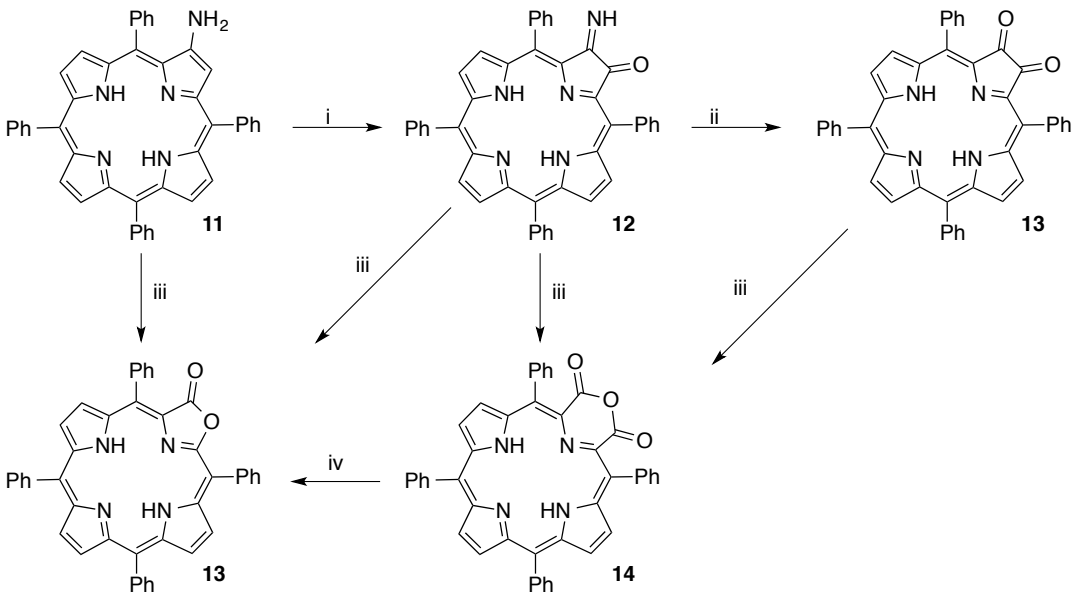

Scheme 1-6. Crossley's introduction of oxygen into the β-pyrrolic position of porphyrins. *Reaction conditions:* i. *hv*, O_2; ii. H^+/H_2O or silica gel; iii. MCPBA; iv. NaOH, H_2O, DMF.

Crossley and King started with *meso*-tetraphenyl-2-aminoporphyrin **11**, obtained by reduction of the corresponding β-nitroporphyin, and then applied a series of oxidative conditions to modify the periphery of the macrocyle.[40] Such conditions involved the photo-oxidation of β-aminoporphyrin **11** to yield the corresponding 2-imino-3-oxochlorin **12**. Upon hydrolysis, **12** was converted into 2,3-dioxochlorin **13**. Oxidation using MCPBA under Baeyer-Villiger conditions formed **13**, while the oxidation of **13** using MCPBA yielded a pyrrole-modified containg a six membered ring, a 2,3a-dioxo-3a-homo-2-oxachlorin **14**. Lactone **13** was produced as the result of an attempted ring-opening reaction of **14**.

The reactions above demonstrated the ability to synthesize pyrrole-modified porphyrins from macrocycles with modifications at the periphery. This was expanded on the "breaking and mending" approach, as explored by the Brückner group. Numerous pyrrole-modified porphyrins became available, containing a range of different non-pyrrolic heterocycles (Scheme 1-7).

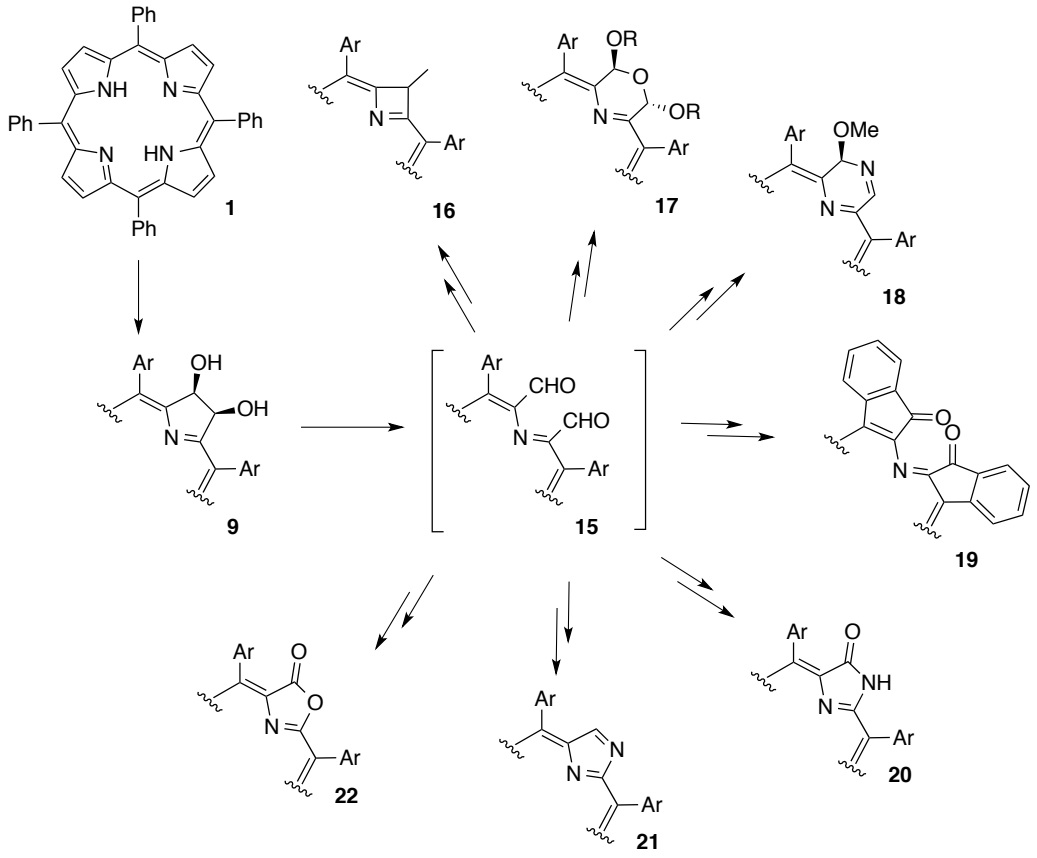

Scheme 1-7. Pyrrole-modified chlorins achieved via the "breaking and mending" of porphyrins strategy.

The "breaking and mending" approach most frequently utilizes diolchlorin **9** as starting material. The diolchlorins produced are exposed to oxidative conditions, for instance, involving the use of $NaIO_4$ or $Pb(OAc)_4$, to cleave the β,β'-carbon bond of the diol to form bisaldehyde secochlorins **15** (Scheme 1-7). This can be considered the "breaking" portion of the "breaking and mending" approach. The mending portion of this methodology, then, comes from the ensuing sequence of reactions that can be induced under a variety of reaction conditions.

Specific examples include the formation of a four-membered azete **16** from a five-membered pyrrole.[31] Also, other reactions result in the ring expansion of a five-membered pyrrole in the porphyrin into a six-membered ring, forming compounds such as morpholine **17**

and pyrazine **18**.[41-44] Another synthetic route to a pyrrole-modified porphyrin includes the formation of an indaphyrin **19** via the application of acid to the bisaldehyde secochlorin **15** in the absence of a nucleophile.[45] Further, the formation of heterocyclic porphyrinoids, such as a porpholactam **20**, imidazoloporphyrin **21**, and porpholactone **22** can be accomplished by replacing a β-carbon with a heteroatom along multi-step sequences.[41, 46-48]

In addition to these modification strategies, multiple total synthesis routes are also available to produce pyrrole-modified porphyrins.

1.5 Optical Properties of Porphyrins and Chlorins

The planar, rigid, 18 π-electron aromatic system of porphyrins imparts their observed electronic and spectroscopic properties. Principally, free-base porphyrins have UV-visible spectra that are characterized by the presence of four absorption bands (Q-bands) between 500-600 nm. Free-base porphyrins exhibit a decreasing order of intensity with respect to the Q-bands, in which the longest wavelength absorption band, the λ_{max}, is the least intense Q-band. Further, free-base porphyrins are characterized by a very intense Soret band, which occurs in the near ultraviolet region, usually between 400-500 nm ($\varepsilon > 10^5$ M^{-1} cm^{-1}) (Figure 1-3).

Similar to free-base porphyrins, free-base chlorins possess a Soret band and four Q-bands. However, unlike free-base porphyrins, free-base chlorins have a λ_{max} Q-band that is the most intense (Figure 1-3). Typically, a broadening in the Soret band and Q-bands of the UV-visible spectra is also observed; this reflects the larger conformational flexibility of this chromophore. Further, free-base chlorins, depending on the particular chlorin, may exhibit a bathochromic shift in the λ_{max} when compared to the parent porphyrin.

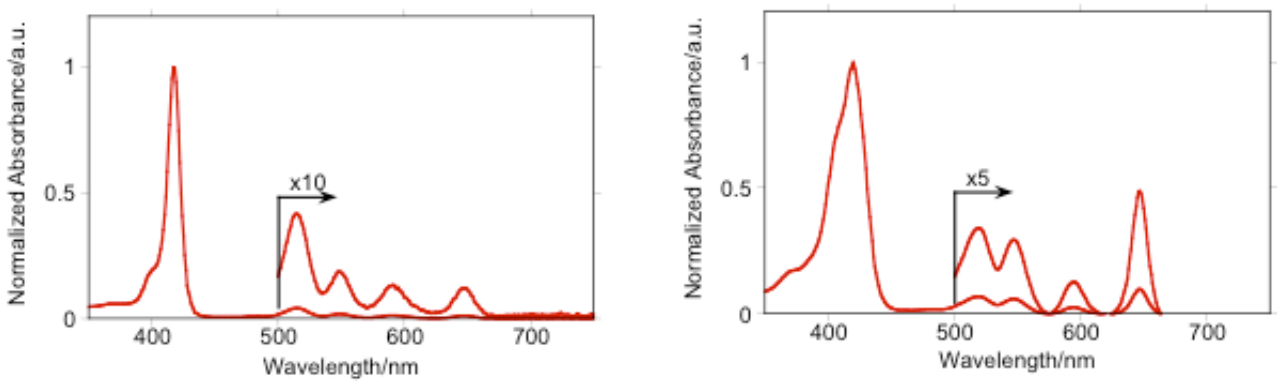

Figure 1-3. UV-visible absorption spectra of a porphyrin (left) and chlorin (right)

The insertion of a metal into the porphyrin or chlorin chromophore alters their optical spectra. Ideally, upon the insertion of a metal, the symmetry of the chromophore will be altered from exhibiting two-fold symmetry to four-fold symmetry, which is reflected in the UV-vis spectra. In porphyrin spectra, the four side bands are diminished into two Q-bands upon metallation. Moreover, the λ_{max} becomes hypsochromically shifted in comparison to its free-base analogue. However, the Soret band remains in the near ultraviolet region between 400-500 nm. The same principal effect is observed for a metal insertion into a chlorin chromophore; the metallated chlorin species will still exhibit a λ_{max} as the most intense Q-band.

In the late 1950's, Gouterman *et al.* rationalized the spectroscopic properties of porphyrins.[49] The absorption spectra of porphyrins can be explained by their electronic frontier orbital transitions.

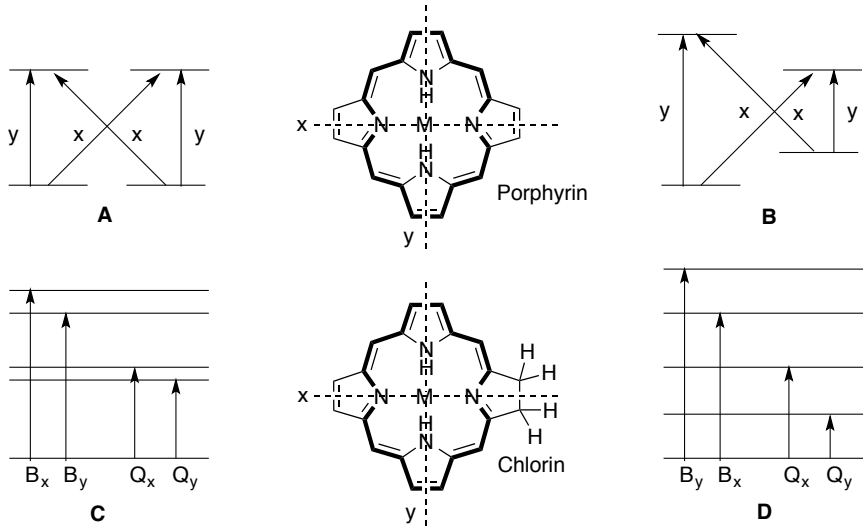

Figure 1-4. A schematic representation of the two HOMOs and two LUMOs (**A**,**B**) and corresponding electronic transition (**C**,**D**); porphyrins with high degeneracy (**A**,**C**) and low degeneracy (**B**,**D**).

Gouterman's four orbital model explains that π to π* transitions give rise to the Soret and Q-bands of the chromophore and proposes that the longest wavelengths at which the porphyrin chromophore absorbs light corresponds to the HOMO-LUMO (Highest Unoccupied Molecular Orbital—Lowest Unoccupied Molecular Orbital) energy gap.[63,64] Alteration to the macrocycle, via modification to the periphery, the *meso*- or β-positions, or by insertion of a metal alters the relative energies of the electronic transitions due to the alteration of the symmetry of the chromophore.[49]

Free base porphyrins, such as TPP, exhibit low D_{2h} symmetry as a result of the presence of opposing nitrogen-bonded inner hydrogens. Defining the x-molecular axis as running through the central nitrogen electron lone pairs, and the y-molecular axis as running through the central N-H bonds, the D_{2h} symmetry of free base porphryins implies that the axes are not equivalent. This means that there is no degeneracy resulting from the excited states from x- or y- polarized

orbital transitions (Figure 1-4). The lack of degeneracy results in spectroscopic transitions split between distinctive x and y bands with Q-allowed transitions.

Moreover, the degeneracy of the HOMOs and LUMOs for a porphyrin with a D_{4h} point group, such as observed with a metalloporphyrin, occurs due to the symmetry of the macrocycle and exemplifies the four excited electronic transitions of a porphyrin (Figure 1-4A).[49-51] The HOMO-LUMO transitions for the D_{4h} point group are split into two high (short wavelength B_x and B_y) and two low (long wavelength Q_x and Q_y) energy transitions, in which high energy transitions are strongly optically allowed with zero probability for a low energy transition.[49-51]

For a chlorin, resulting from the reduction at the β,β'-position of the macrocycle, the symmetry is further decreased from the parent chromophore (Figure 1-4B). The orbitals containing most of the electron density on the β,β'-carbons are most affected by the modulation to the parent chromophore as observed in the induced optical transitions (Figure 1-4C,D). In other words, the HOMO-LUMO gap is decreased and resulting in a more symmetry-allowed HOMO-LUMO transition. This explains the increased intensity of the λ_{max}, as well as the bathochromic shift that is sometimes observed in chlorin spectra.[49-51]

1.6 Application of Porphyrins and Chlorins: Photodynamic Therapy

Porphyrins, their analogues, and their metal complexes, have found a number of technical and medicinal applications. For example, they have been utilized as sensitizer dyes in the photodynamic therapy treatment (PDT) of cancer and the treatment of age-related macular degeneration,[1] as high pH sensor dyes,[52] as pressure sensitive paints (PSP) used in aeronautics R&D, [53-55] and as chromophores in artificial light harvesting systems.[56]

1.6.1 Photodynamic Therapy

Photodynamic therapy (PDT) capitalizes on the optical properties of porphyrins and applies them to use in biological systems in an attempt to induce a desired biological effect. PDT uses a combination of light and a photosensitizing compound (or drug) to eradicate cancerous or other malignant and unwanted tissues.[57-59] PDT has been employed for use with removing certain cancers (e.g. breast cancer), as well as, treating psoriasis, and age-related macular degeneration.

The process of PDT involves systematic intravenous administration of a photosensitizer of negligible dark toxicity, followed by (ideally) localization of the photosensitizer in the target tissue, and ensuing irradiation using an appropriate wavelength of light (Figure 1-5). The photosensitizer drug, via photophysical processes, generates reactive oxygen species (ROS), primarily cytotoxic singlet oxygen, which induces oxidative stress to the cell and this, in turn induces apoptosis in the areas where the drug localized, eradicating the affected cell.[60]

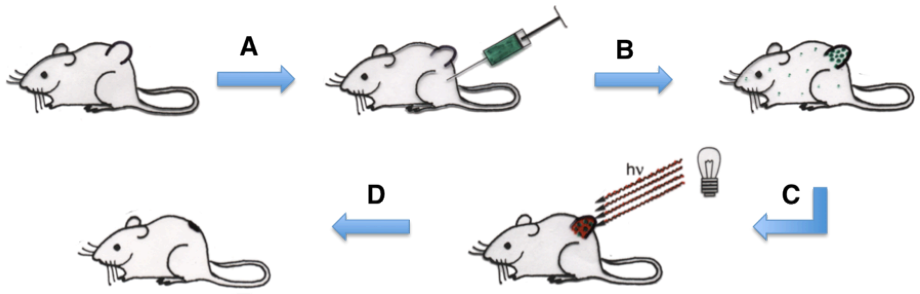

Figure 1-5. Process of PDT: administration (**A**), localization (**B**), irradiation (**C**) and eradication (**D**). Figure from Ref. 58.

The depth of the penetration of light through tissue is dependent upon the wavelength of the light (Figure 1-6). [60] The depth of the penetration of light is also limited by other factors, including, the absorption by endogenous chromophores (primarily hemoglobin), as well as, the optical scattering that occurs within the tissue.[60] These factors considered, an ideal

photosensitizer should then not only remain biologically inactive (or of minimally significant biological activity) until activated by light, but also absorb light in the red or near-IR, and be able to produce singlet oxygen.[60]

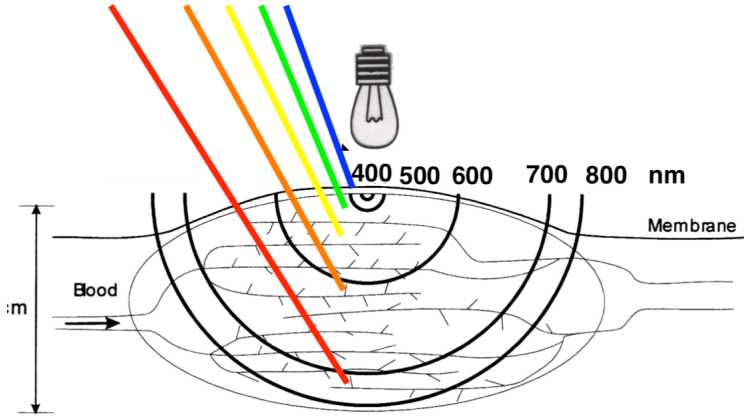

Figure 1-6. Dependence of the penetration of light as a function of wavelength. Figure adopted from Ref. 60.

A modified Jablonski diagram, depicted below in Figure 1-7, effectively illustrates the photophysical processes involved in PDT. First, the absorption of light causes the singlet ground state (S_0) photosensitizer to become excited into an excited singlet state (S_n) (pathway 1). Next, fluorescence may occur as the molecule relaxes back to its ground state (pathway 2), or the molecule can relax back to its ground state non-radiatively through an internal conversion process (pathway 3). These pathways are quantum-chemically spin allowed.

Another process, a quantum-chemically spin-forbidden process, allows the excited molecule to undergo inversion and populate the triplet state. This non-radiative route called inter-system crossing (ISC, pathway 4) and can readily occur in porphyrins. They therefore generally possess high triple state quantum yields. Moreover, the excited chromophore can relax to its ground state via phosphorescence (pathway 5), or via a spin and energy exchange process with another triplet-excited species (pathway 6). The spin exchange pathway, which can occur with

molecular oxygen, can result in the generation of triplet oxygen ($^3O_2$). Singlet oxygen ($^1O_2$) being very reactive and thus toxic, can induce a variety of biological reactions from its interaction with biological substrates. [58, 59]

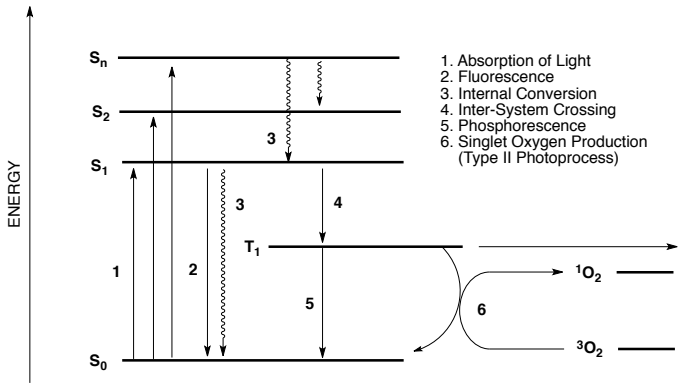

Figure 1-7. Modified Jablonski diagram for a photosensitizer. Figure from Ref. 73.

1.7 References

1) *The Porphyrin Handbook*; Kadish, K. M.; Smith, K. M.; Guilard, R., Eds; Academic Press: San Diego, 2000, 2003; Vol. 1-20.

2) *The Colours of Life*; Milgrom, L. R.; Oxford University Press: New York, **1997**.

3) Brückner, C.; Dolphin, D. *Tetrahedron Lett*. **1995**, 36, 3295-3298.

4) Kaim, W.; Schwederski, B. *Bioinorganic Chemistry: Inorganic Elements in the Chemistry of Life* John Wiley & Sons Ltd: West Sussex, 1994.

5) Rothemund, P. *J. Am. Chem. Soc.* **1936**, *58*, 625.

6) Adler, A. D.; Longo, F. R.; Finarelli, J. D.; Goldmacher, J.; Assour, J.; Korsakoff, L. *J. Org. Chem.* **1967**, *32*, 476.

7) Lindsey, J. S.; Schreiman, I. C.; Hsu, H. C.; Kearney, P C.; Marguerettaz, A. M. *J. Org. Chem* **1987**, *52*, 827-36.

8) Lindsey, J. S.; Schreiman I. C., *Tetrahedron Lett.* **1986**, *27*, 4969-4970.

9) McCarthy, J. R. Novel Macrocycles by Modification of the β, β'-Position of porphyrins. PhD thesis, University of Connecticut, Storrs, 2003.

10) Shioi, Y. In *Chlorophylls and Bacteriochlorophylls*; Grimm, B., Porra, R. J., Rüdinger, W., Scheer, H., Eds.; Springer: Dordrecht, NL, 2006, p 123-131.

11) Whitlock, H. W., Jr.; Hanauer, R.; Oester, M. Y.; Bower, B. K. *J. Am. Chem. Soc.* **1969,** *91*, 7485-7489.

12) Fischer, H.; Eckoldt, H. *Liebigs Ann. Chem.* **1940**, *544*, 138-162.

13) Chang, C. K.; Sotitiou, C.; Wu, W. *J. Chem. Soc.*, *Chem. Commun.* **1986**, 1213-1215.

14) Bonnett, R.; nizhnik, A. N.; White, S. G.; Berenbaum, M. C. *J. Photochem. Photobiol. B* **1990**, *6*, 29-37.

15) Meunier, I.; Pandey, R. K.; Walker, M. M.; Senge, M. O.; Dougherty, T. J.; Smith, K. M. *Bioorg. Med. Chem. Lett.* **1992**, *2*, 1575-1580.

16) Pandey, R. K. *Proceed. of SPIE* **1992**, *1645*, 264-273.

17) Pandey, R. K.; Shiau, F. Y.; Isaac, M.; Ramaprasad, S.; Dougherty, T. J.; Smith, K. M. *Tetrahedron Lett.* **1992**, *33*, 7815-7818.

18) Smith, K. M.; Pandey, R. K.; Shiau, F. Y.; Smith, N. W.; Iakovides, P.; Dougherty, T. J. *Proceed. of SPIE* **1992**, *1645,* 274-283.

19) Gerzevske, K. R.; Pandey, R. K.; Smith, K. M. *Heterocycles* **1994**, *39*, 439-443.

20) Pandey, R. K.; Shiau, F.-Y.; Sumlin, A. B.; Dougherty, T. J.; Smith, . M. *Bioorg. Med. Chem. Lett.* **1994**, *4*,1263-1267.

21) Kozyrev, A. N.; Dougherty, T. J.; Pandey, R. K. *Tetrahedron Lett.* **1996,** *37*, 3781-3784.

22) Zheng, G.; Dougherty, T. J.; Pandey, R. K. *J. Org. Chem.* **1999**, *64*, 3751-3754.

23) Chen, Y.; Mendforth, C. J.; Smith, K. M.; Alderfer, J.; Dougherty, T. J.; Pandey, R. K. *J. Org. Chem.* **2001**, *66*, 3930-3939.

24) McCarthy, J. R.; Bhaumik, J.; Merbouh, N.; Weissleder, R. *Org. Biomol. Chem.* **2009**, *7*, 3430-3436.

25) Brückner, C.; Dolphin, D. *Tetrahedron Lett.* **1995**, *36*, 9425-9428.

26) Brückner, C.; Rettig, S. J.; Dolphin, D. *J. Org. Chem.* **1998**, *63*, 2094-2098.

27) Samankumara, L. P.; Zeller, M.; Krause, J. A.; Brückner, C. *Org. Biomol. Chem.* **2010**, *8*, 1951-1965.

28) Starnes, S. D.; Rudevich, D. M.; Rebek Jr., J. *J. Am. Chem. Soc.* **2001**, *123*, 4659-4669.

29) Shultz, D. A.; Gwaltney, K. P.; Lee, H. *J. Org. Chem.* **1998**, *63*, 769-774.

30) Zhou, X.; Chan, K. S. *J. Org. Chem.* **1998**, *63*, 99-104.

31) Banerjee, S.; Hyland, M. A.; Brückner, C. *Tetrahedron Lett.* **2010**, *51*, 5405-4508.

32) Lindsey, J.S.; Mass, O.; Chen, C.-Y. *New J. Chem.* **2011**, *35*, 511-516.

33) Krayer, M.; Yang, E.; Kim, H.-J.; Kee, H. L.; Deans, R. M.; Sluder, C. E.; Diers, J. R.; Kirmaier, C.; Bocian, D. F.; Holten, D.; Lindsey, J. S. *Inorg. Chem* **2011**, *50*, 607-4618.

34) Balasubramanian, T.; Strachan, J.-P.; Boyle, P. D.; Lindsey, J.S. *J. Org. Chem.* **2000**, *65*, 7919-7929.

35) Strachan, J.-P.; O'Shea, D. F.; Balasubramanian, T.; Lindsey, J. S. *J. Org. Chem.* **2000**, *65*, 3160-3172.

36) Arnott, D. M.; Harrison, P. J.; Henderson, G. B.; Sheng, Z.-C; Leeper, F. J.; Battersby, A. R. *J. Chem. Soc. Perkin Trans. I* **1989**, 265-278.

37) Harrison, P. J.; Fookes, C. J. R.; Batersby, A. R. *J. Chem. Soc.*, *Chem. Commun.* **1981**, 797-799.

38) Harrison, P. J.; Sheng, Z.-C.; Fookes, C. J. R.; Battersby, A. R. *J. Chem. Soc.*, *Perkin Trans. I* **1987**, 1667-1678.

39) Snow, R. J.; Fookes, C. J. R.; Battersby, A. R. *J. Chem. Soc.*, *Chem. Commun.* **1981**, 524-526.

40) Crossley, M. J.; King, L. G. *J. Chem. Soc., Chem. Commun.* **1984**, 920-922

41) McCarthy, J. R.; Jenkins, H. A.; Brückner, C. *Org. Lett.* **2003**, *5*, 19-22.

42) Brückner, C.; Götz, D. C. G.; Fox, S. P.; Ryppa, C.; McCarthy, J. R.; Bruhn, T.; Akhigbe, J.; Banerjee, S.; Daddario, P.; Daniell, H. W.; Zeller, M.; Boyle, R. W.; Bringmann, G. *J. Am. Chem. Soc.* **2011**, *133*, 8740-8752.

43) Dean, M. L., Ph.D. thesis, University of Connecticut, 2011.

44) Zarate, G., M.S. Thesis, University of Connecticut, 2010.

45) McCarthy, J. R.; Hyland, M. A.; Brückner, C. *Org. Biomol. Chem.* **2004**, *2*, 1484-1491.

46) Akhigbe, J.; Haskoor, J.; Zeller, M.; Brückner, C. *Chem. Commun.* **2011**, *47*, 8599-8601.

47) Akhigbe, J.; Peters, G.; Zeller, M.; Brückner, C. *Org. Biomol. Chem.* **2011**, *9*, 230-2313.

48) Brückner, C.; Ogikubo, J.; McCarthy, J. R.; Akhigbe; Hyland, M. A.; Daddario, P.; Worlinsky, J. L.; Zeller, M.; Engle, J. T.; Ziegler, C. J.; Ranaghan, M. J.; Sandberg, M. N.; Birge, R. R. *J. Org. Chem.* **2012**, *77*, 6480-6494.

49) Gouterman, M., Study of Effects of Substituents on the Absorption Spectra of Porphyrins. *J. Chem. Phys.* **1959**, *30*, 1139-1161.

50) Gouterman, M. In *The Porphyrins*; Dolphin, D., Ed.; Academic Press: New York, San Francisco, London, 1978; Vol. III, p 1-165.

51) Gouterman, M. *J. Mol. Spectrosc.* **1961**, *6*, 138-163.

52) Buchler, J. W. In *Porphyrins*; Dolphin, D., Ed. 1978; Vol. 1, p 389-483.

53) Gouterman, M.; Callis, J.; Dalton, L.; Khalil, G.; Mebarki, Y.; Cooper, K. R.; Grenier, M. *Meas. Sci. Technol.* **2004**, *15*, 1986-1994.

54) Zelelow, B.; Khalil, G. E.; Phelan, G.; Carlson, B.; Gouterman, M.; Callis, J. B.; Dalton, L. R. *Sens. Actuators, B* **2003**, *96*, 304-314.

55) Khalil, G. E.; Costin, C.; Crafton, J.; Jones, G.; Grenoble, S.; Gouterman, M.; Callis, J. B.; Dalton, L. R. *Sens. Actuators, B* **2004**, *97*, 13-21.

56) Chen, 1.; Akhigbe, J.; Brückner, C.; Li, C. M.; Lei, Y. *J. Phys. Chem. C* **2010**, *114*, 8633-8638.

57) MacDonald, I. J.; Dougherty, T. J. *J. Porphyrins Phthalocyanines* **2001**, *5*, 105-129.

58) Josefsen, L. B.; Boyle, R. W. *Theranostics* **2012**, *2*, 916-966.

59) DeRosa, M. C.; Crutchley, R. J. *Coord. Chem Rev.* **2002**, *233-234*, 351-371.

60) Sternberg, E. D.; Dolphin, D; Brückner, C. *Tetrahedron* **1998**, *54*, 4151-4202.

61) Guldi, D. M.; Mody, T. D.; Gerasimchuk, N. N.; Magda, D.; Sessler, J. L. *J. Am. Chem. Soc.* **2000**, *122*, 8289-8298.

2. *meso*-Aryl-3-alkyl-oxachlorins

2.1 Introduction

2.1.1 Porpholactones

Several routes are available for the transformation of the β-β'-bond into a lactone moiety, forming what is known as a porpholactone **3**.[1-6] One such pathway involves the use of an OsO_4-mediated dihydroxylation of *meso*-tetraarylporphyrin **1** to produce diolchlorin **2** which is subsequently oxidized in a single step by MnO_4^- to produce **3** (Scheme 2-1).[2] The source of MnO_4^-, which is added in excess, can be added to the reaction in the form of powdered, suspended $KMnO_4$ in an organic solvent, or added in the presence of a phase-transfer reagent, heterogenized on silica gel, or added in the form of cetyltrimethylammonium permanganate (CTAP).[2,7]

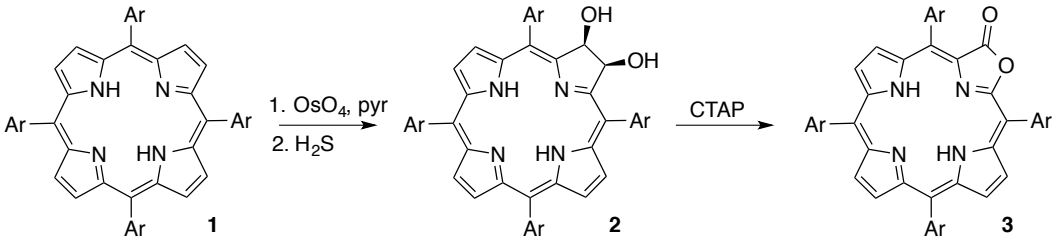

Scheme 2-1. Synthesis of porpholactones **3** by MnO_4^- mediated oxidation of 2,3-dihydroxychlorins 2.

Porpholactones, have been found to be of use as model compounds for chlorin-type prosthetic groups, use as high pH sensors, and use as a component in pressure sensitive paints.[8,9] [10-14] Further, the conversion of *meso*-tetraarylporphyrins to

porpholactones **3** proved to be a key conversion for the preparation of an oxazole moiety into the macrocycle.

Chlorin chromophores, especially oxazolochlorin derivatives, are often highly unstable when exposed to oxidative conditions. The instability of this class of chromophores limits the ability to study and exploit the properties of these compounds. The susceptibility of this class of compounds is exemplified with the oxidation at the α-position of **4**, synthesized by reduction of **3**, after exposure to air and light to form porpholactol **5** (Scheme 2-2).[13] Subsequent OsO_4-mediated dihydroxylation of hemiacetal **5** results in the formation of lactone **3**.[13]

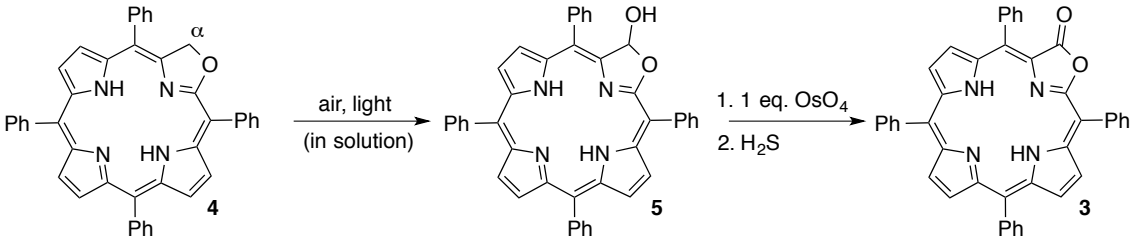

Scheme 2-2. Extemporaneous oxidations at the α-carbon of oxazolochlorins.

Previous work by the Lindsey group involving the total synthesis of chlorins and bacteriochlorins demonstrated that the addition of a geminal dimethyl moiety to the chlorin and bacteriochlorin chromophores stabilized these classes of compounds.[15,16] This prompted us to investigate the effect of the addition of alkyl substituents on the stability of oxazolochlorins. This chapter explores alkylation and reduction of porpholactones using alkyl-Grignard reagents.

2.2 Results and Discussion

2.2.1 Synthesis of Alkyloxazolochlorins

Addition of alkyl (ethyl, *i*-propyl) Grignard reagents to the zinc(II) complex of porpholactone **3Zn** under anhydrous conditions results in the formation of a more polar product. An aqueous acidic work-up using a strong enough acid to demetalate the zinc complexes provided free base porphyrinoids with a chlorin-like UV-visible spectra as the main products in good to satisfactory yields. The HR–MS (ESI+) of these compounds suggested their composition to be derived from the parent porpholactone to which a single equivalent of ethane and propane was added, respectively. Their ^{1}H, ^{13}C NMR, and IR spectra also confirmed the loss of the lactone functional group and the presence of an alkyl chain attached to the oxazole moiety. These spectroscopic data and their similarity to those of the porpholactol identified these products as the alkylated hemiketals **6**. The use of 2 to 3 equivalents of Grignard reagent was found to provide the highest yields of product. The reaction is rapid (5-20 mins at ambient temperature), and can be scaled up to 600 mg of **3Zn**, 0.62 mmol, whereby the addition of the Grignard reagent at lower temperatures, –78°C for ^{i}PrMgBr and –45°C for EtMgCl, was found beneficial for this substrate). The presence of the 'protecting group' zinc(II) is obligatory as the alkylation of free base porpholactones failed.

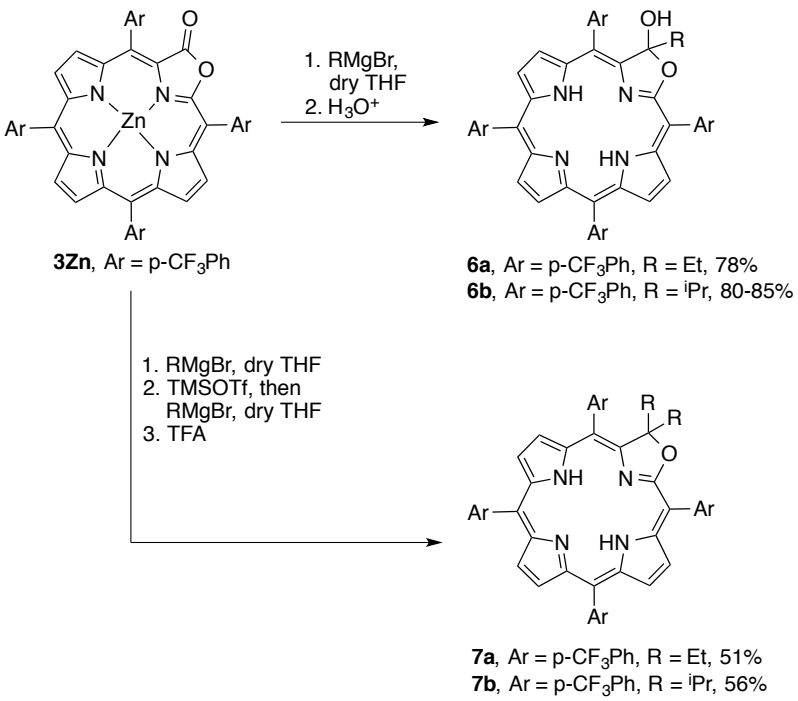

Scheme 2-3. Synthesis of mono- and bis-alkyloxazolochlorins by alkyl-Grignard addition to porpholactone **3Zn**.

Even the use of a large excess of Grignard reagent (e.g., 15-fold molar excess) did not generate more than traces of the corresponding bis-alkylated systems. The use of the more electron withdrawing 4-CF_3Ph-derivatives also did not improve the yield of formation of the bisalkylated products. However, reaction of **3Zn** with an alkyl-Grignard reagent, followed by reaction of the crude zinc complex of **6** with a Lewis acid and further addition of alkyl-Grignard reagent furnished the dialkyl-derivatives **7** in satisfying yields (Scheme 2-3). We screened a number of Lewis acids ($BF_3{\cdot}OEt_2$, TMSOTf, $Sc(OTf)_3$, $InCl_3$, $Ti(O^iPr)_4$, and $TiCl_4$) for their ability to catalyze this reaction and found TMSOTf to be the best choice.

We have also tested *i*-propyl lithium as an alkylating agent. The reaction formed the expected mono-alkylated compounds. However, the experimental conditions (reaction

temperatures of –78°C were required for the reagent) and the precautions associated with using the alkyllithium reagent were not offset by higher yields, a larger fraction of bisalkylated product, or cleaner reactions when compared to the Grignard reactions. Thus, we did not develop this route toward alkyloxazolochlorins.

The oxazolochlorins of types **6** and **7** are distinguished by excellent solubilities, unlike other mono-alkyloxazolochlorins that were explored.

2.3 Optical Properties of Alkyloxazolochlorins

Benchmark compound free base porpholactol **5** possesses a chlorin-type UV-visible absorption spectrum (λ_{max} = 646 nm).[2] The spectra of the mono-alkylated analogues (**6a**: λ_{max} = 649 nm, **6b**: λ_{max} = 650 nm) are nearly indistinguishable from that of the non-alkylated species (porpholactol). Likewise, the optical spectra of the ethyl and *i*-propyl derivatives were indistinguishable from each other. The bis-alkyloxazolochlorins **7** possess λ_{max} values that are similar to those of the dehydroxylated monoalkyloxazolochlorins discussed (Figure 2-1).

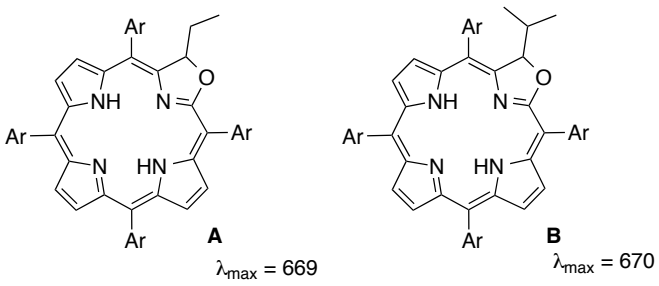

Figure 2-1. Monoalkyloxazolochlorins and corresponding λ_{max} values ; Ar = *p*-CF_3Ph.

However, the shapes of their Soret bands and the peak positions of the remaining Q-bands are distinctly different. Also, the UV-visible spectra of the bis-alkyloxazolo-

chlorins possess almost 50% lower extinction coefficients compared to the corresponding mono-alkylated species.

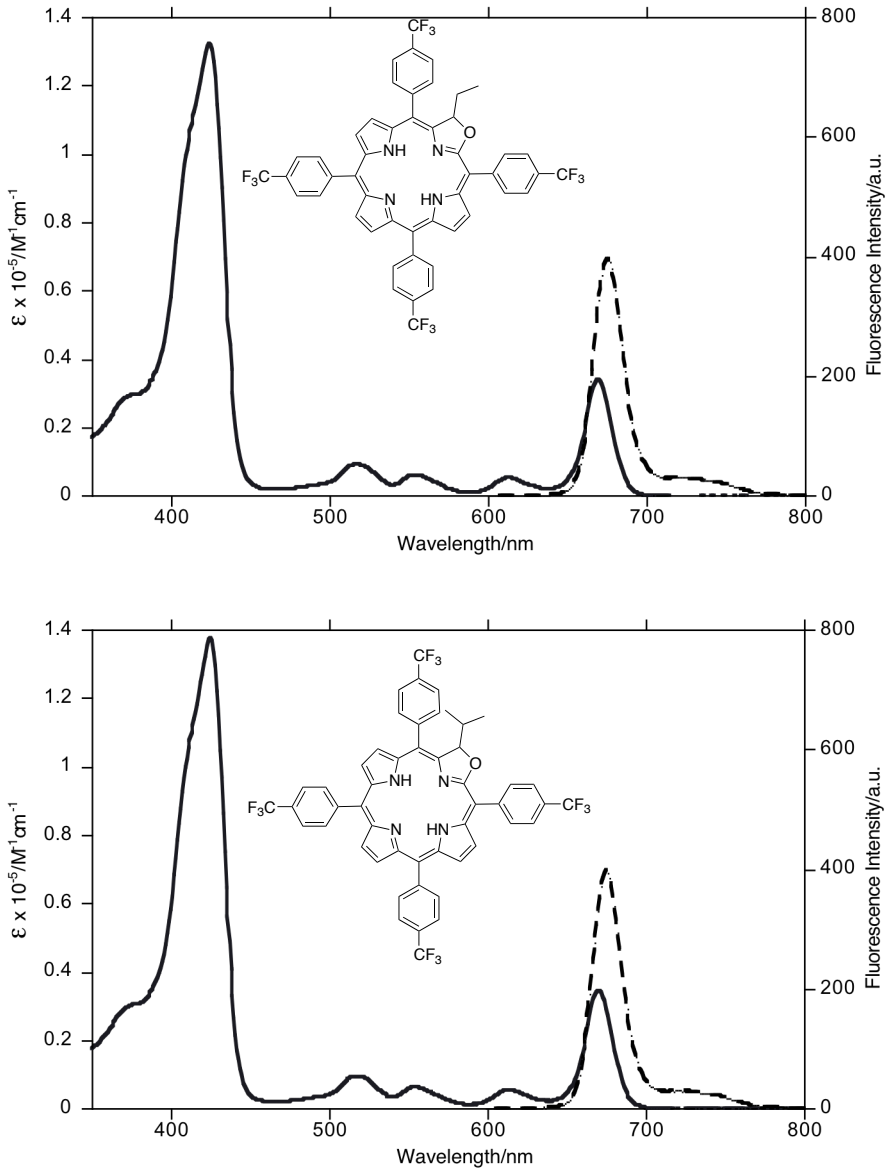

Figure 2-2. UV-vis (solid trace) spectra and fluorescence (broken trace) spectra of **A** (top) and **B** (bottom); Ar = *p*-CF_3Ph.

The fluorescence yields are in the range of 0.27 to 0.36. The fluorescence emission spectra of the alkyloxazolochlorins are all chlorin-type (Figure 2-2), with the small Stokes' shift characteristic for porphyrins.

2.4 Conclusions

The addition of Grignard reagents to the porphyrin-like *meso*-tetraarylporpholactones resulted in the formation of mono- and bis-alkylated oxazolochlorins. The oxazolochlorins possess chlorin-like optical properties that are slightly modulated depending on the nature of the substituents located on the sp^3-hybridized carbon α to the oxazole oxygen. Since porpholactones are readily accessible in gram-scales and the key reactions were demonstrated at gram or half-gram scales, this methodology offers straightforward access to significant quantities of a class of stable chlorin-like chromophores that are endowed with somewhat tunable optical spectra. This tunability, the reasonably high fluorescence quantum yields and the facile derivatization of the chromophores encourage the further study and application of this unique porphyrinoid class. Experiments to test their applicability as light-harvesting devices and in photomedicine are currently underway.

2.5 Experimental Section

2.5.1 Instruments and Materials

[*meso*-Tetraarylporpholactonato]Zn(II) **3Zn** was synthesized as reported in the literature.[2] Flash column chromatography was performed manually in glass columns or on an automated flash chromatography system, on normal-phase silica (solvents used are

indicated; isochratic eluation modes). The crude products were dry-packed onto silica gel in a pre-column unless noted otherwise. The fluorescence quantum yileds (ϕ) were determined relative to those of *meso*-tetraphenylporphyrin (ϕ = 0.11 in benzene, calculated to be 0.09 in CH_2Cl_2); $\lambda_{Excitation} = \lambda_{Soret}$. For details of the instruments used, see *List of Instruments*.

2.5.2 Preparation and Characterization

***meso*-Tetrakis(4-trifluoromethylphenyl)-3-ethyl-3-hydroxy-2-oxachlorin (6a). General procedure for the conversion of lactone 3Zn to hemiketal 6.** For a typical reaction, a N_2-flushed, oven dried 50 mL round bottom flask was loaded with [*meso*-tetrakis(trifluoromethylphenyl)-2-oxa-3oxoporphyrinato]Zn(II) (**3Zn,** 113 mg, 0.117 mmol) dissolved in dry THF (15 mL). Then, 2 equiv of EtMgBr (2M solution in THF, 117 μL) was slowly added at –45°C. For best yield, the reaction should be maintained at –45°C until it is quenched. The reaction progress was monitored using UV-vis spectroscopy (disappearance of the band at ~600 nm and development of a band at ~625 nm). The reaction was completed within 15 min. Upon completion, the reaction was quenched by addition of a saturated aq. NH_4Cl solution (2-3 mL). The mixture was transferred into a 250 mL separatory funnel and washed with saturated aq. NH_4Cl, and the chlorin was extracted with CH_2Cl_2. Note: it appears critical to assure that all Grignard reagent is quenched; repeated aq. NH_4Cl washes may be necessary. Crude **6aZn** was dissolved in THF (15 mL) and stirred, and 6 M aq HCl (2-3 mL) was added. The reaction was stirred for ~2 hrs. The reaction progress was monitored by UV-vis spectroscopy. Upon disappearance of the metallochlorin spectrum of a neutralized aliquot, the green

reaction mixture was transferred into a separatory funnel and a saturated aq. $NaHCO_3$ solution is added (Caution, foam!). CH_2Cl_2 was added and the organic layer was extracted. The aq. $NaHCO_3$ wash was repeated until the organic layer was pure purple in color. The organic phase was isolated and dried over K_2CO_3. The product **6a** was isolated by column chromatography (silica-50% petroleum ether/CH_2Cl_2) as a purple solid in 78% (85 mg) yield. MW = 934.8 g/mol; R_f = 0.26 (silica-50% petroleum ether 30-60/CH_2Cl_2); UV-vis ($CHCl_3$) λ_{max} (log ε): 419 (5.13), 513 (4.00), 548 (3.99), 595 (3.75), 649 (4.45) nm, Fl λ_{max} ($CHCl_3$, λ_{exc} = 419 nm): 654, 702 nm, ϕ = 0.29; ^{1}H NMR (300 MHz, $CDCl_3$, δ): 8.59 (d, ^3J = 5.1 Hz, 1H), 8.45 (d, ^3J = 3.9 Hz, 1H), 8.42 (d, ^3J = 5.0 Hz, 1H), 8.39 (d, ^3J = 4.6 Hz, 1H), 8.32 (d, ^3J = 4.6 Hz, 1H), 8.18–7.99 (m, 15H), 7.87 (d, ^3J = 8.0 Hz, 1H), 7.77 (d, ^3J = 8.0 Hz, 1H), 3.84 (s, 1H), 2.38–2.29 (m, 1H), 1.92–1.86 (m, 1H), 0.74 (t, ^3J = 7.3 Hz, 3H), –0.63 (s, 1H), –0.99 (s, 1H) ppm; ^{13}C NMR (100 MHz, $CDCl_3$, δ): 163.2, 154.9, 152.3, 151.4, 145.4, 145.2, 142.9, 142.7, 142.3, 141.6, 136.9, 135.3, 134.2, 134.2, 134.0, 134.0, 133.9, 133.8, 131.8, 130.0, 129.9, 127.7, 126.0, 125.7, 125.1, 125.1, 125.0, 124.3, 124.3, 124.1, 124.1, 124.0, 123.9, 123.9, 123.3, 123.3, 123.3, 123.3, 122.8, 120.1, 112.3, 110.7, 99.2, 32.7, 8.57; HR-MS (ESI+ of MH^+, 100% CH_3CN, TOF): *m/z* calc'd for $C_{49}H_{31}F_{12}N_4O_2$: 935.2255, found 935.2236.

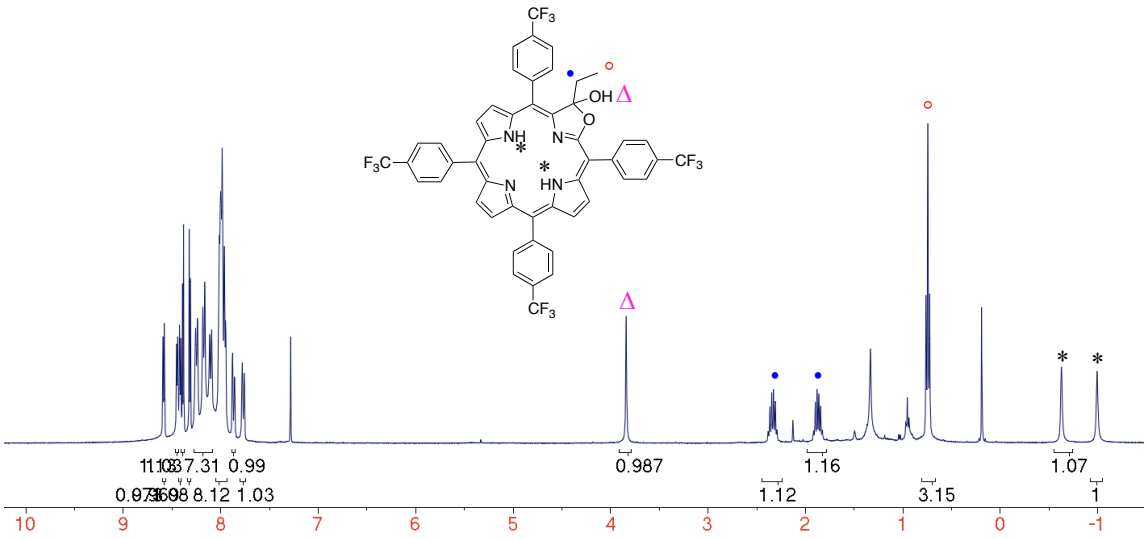

Figure 2-3. Illustrated ^{1}H NMR spectrum (400 MHz, $CDCl_3$) of **6a**.

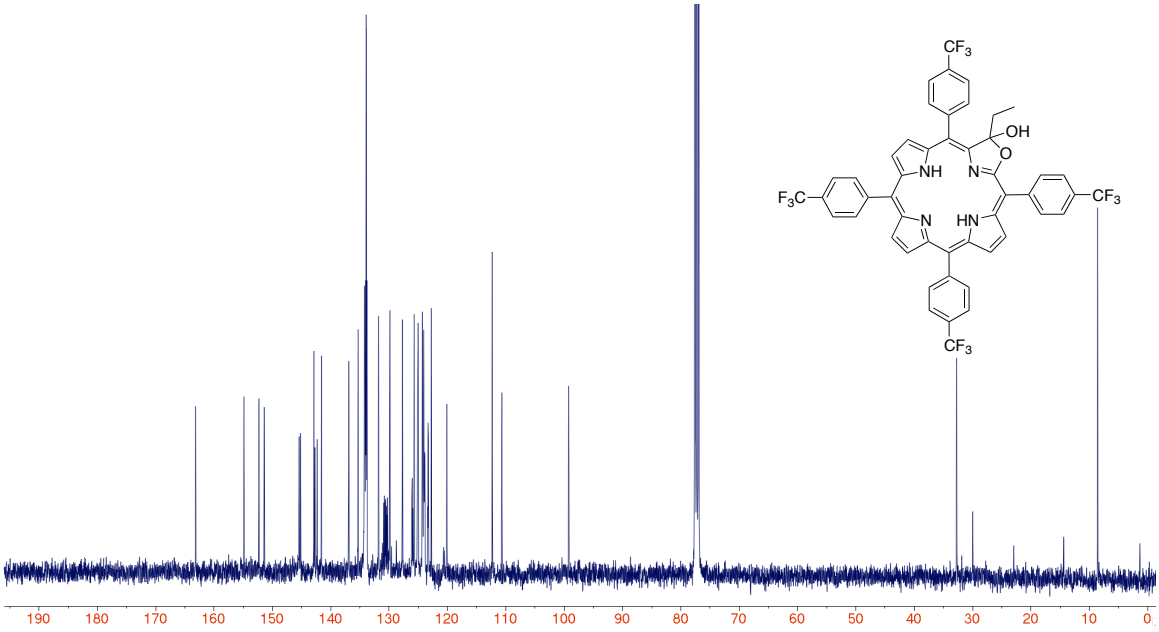

Figure 2-4. ^{13}C NMR spectrum (100 MHz, $CHCl_3$) of **6a**.

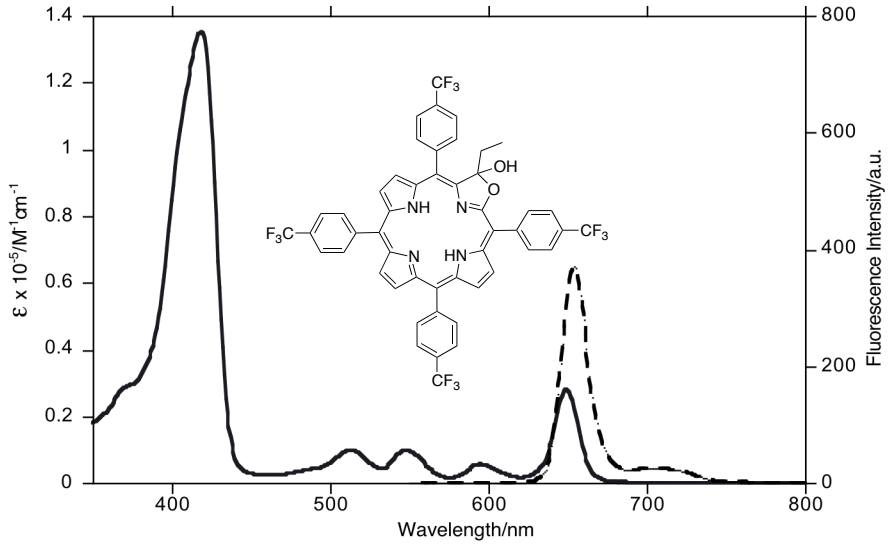

Figure 2-5. UV-vis (solid trace) and fluorescence (broken trace) spectra of **6a** ($CHCl_3$).

***meso*-Tetrakis(4-trifluoromethylphenyl)-3-hydroxy-3-isopropyl-2-oxachlorin (6b).** Prepared from [*meso*-tetrakis(trifluoromethylphenyl)-2-oxa-3-oxoporphyrinato]Zn(II) (**3Zn,** up to 500 mg scale) according to the reaction procedure described for the preparation of **6a**, except the reaction was performed using *i*-PrMgCl (2M solution in THF, 0.515 mL for 500 mg scale) maintained at –78°C. The product **6b** was isolated by chromatography (silica-50% petroleum ether 30-60/CH_2Cl_2) as a purple solid in 80-85% yield (up to 415 mg). MW = 948.8 g/mol; R_f = 0.32 (silica-50% petroleum ether 30-60/CH_2Cl_2); UV-vis ($CHCl_3$) λ_{max} (log ε): 420 (5.24), 513 (4.10), 548 (4.09), 595 (3.88), 650 (4.55) nm; Fl λ_{max} ($CHCl_3$, λ_{exc} = 420 nm): 655, 703 nm, ϕ = 0.36; ^{1}H NMR (300 MHz, $CDCl_3$, δ): 8.57 (d, ^3J = 4.9 Hz, 1H), 8.42 (m, 2H), 8.36 (d, ^3J = 4.5 Hz, 1H), 8.15–7.95 (m, 19H), 3.87 (s, 1H), 2.14–2.08 (m, 1H), 1.28 (d, ^3J = 6.5 Hz, 3H), 0.65 (d, ^3J = 6.7 Hz, 3H), –0.63 (s, 1H), –0.99 (s, 1H) ppm; ^{13}C NMR (100 MHz, $CDCl_3$, δ): 163.2, 154.8, 153.7, 151.3, 145.4, 145.1, 142.8, 142.7, 142.7, 142.4, 141.8, 136.9, 135.3, 134.2,

134.1, 134.0, 133.9, 133.9, 133.9, 133.7, 131.7, 129.8, 127.7, 125.7, 125.0, 124.3, 124.2, 124.2, 124.1, 124.0,124.0, 123.9, 123.8, 123.3, 123.3, 123.2, 122.8, 120.1, 113.6, 110.4, 99.1, 36.4, 17.5, 15.9; HR-MS (ESI+ of MH^+, 100% CH_3CN, TOF): *m/z* calc'd for $C_{50}H_{33}F_{12}N_4O_2$: 949.2412, found 949.2431.

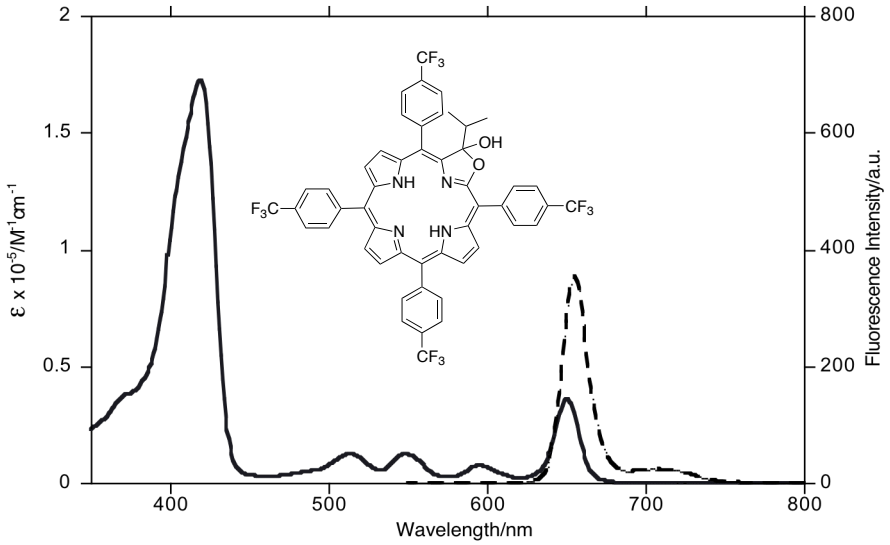

Figure 2-6. UV-vis (solid trace) and fluorescence (broken trace) spectra of **6b** ($CHCl_3$).

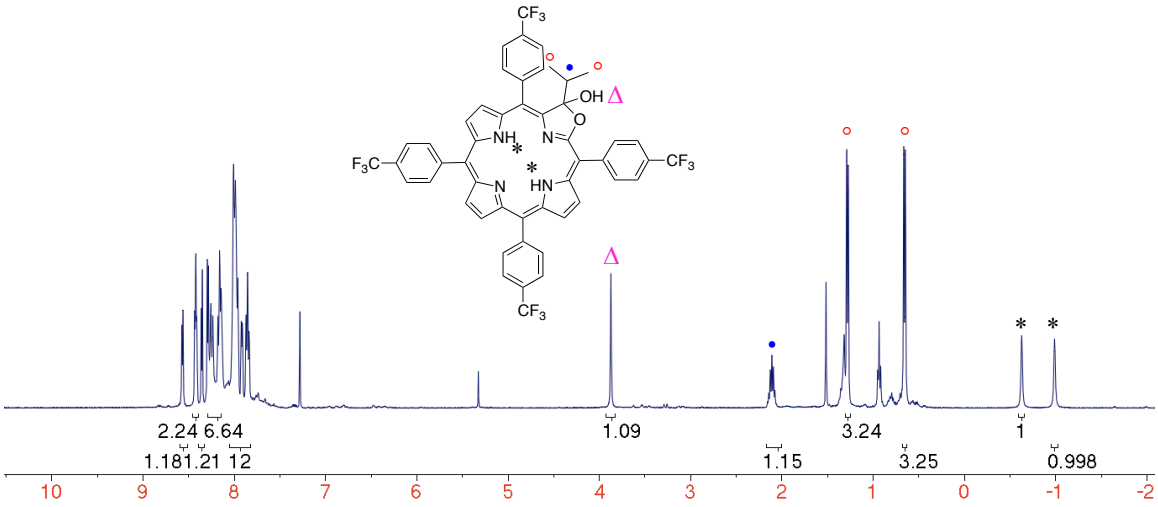

Figure 2-7. Illustrated ^{1}H NMR spectrum (400 MHz, $CDCl_3$) of **6b**.

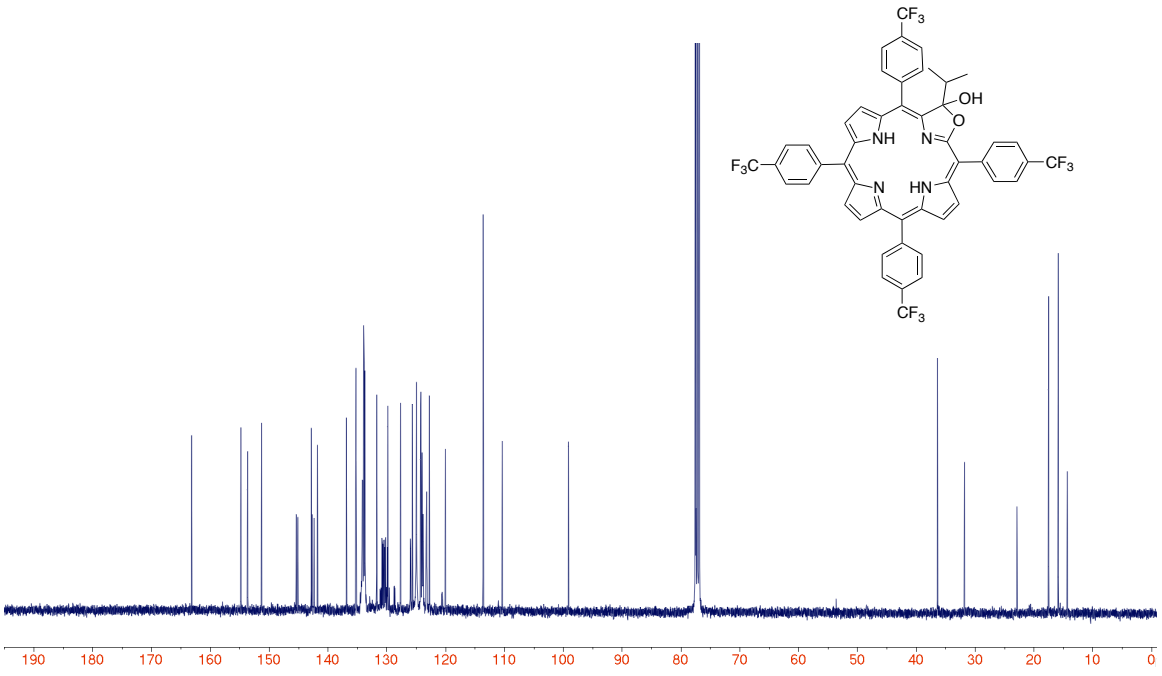

Figure 2-8. ^{13}C NMR spectrum (100 MHz, $CDCl_3$) of **6b**.

***meso*-Tetrakis(4-trifluoromethylphenyl)-3,3-diethyl-2-oxachlorin (7a). General procedure for the conversion of porpholactone 3Zn to bis-alkyloxazolochlorin 7.** Prepared from [*meso*-tetrakis(4-trifluoromethylphenyl)-2-oxa-3-oxoporphyrinato]Zn(II) (**3Zn**, 40 mg, 4.1×10^{-5} mol) and EtMgCl. Step 1: Lactone zinc (II) complex **3Zn** (40 mg, 4.1×10^{-5} mol), was dissolved in dry THF and stirred under N_2 at –45°C and 2 equiv of EtMgCl (2M solution in THF, 0.041 mL) were added. The reaction progress was monitored using UV-visible spectroscopy (development of an intense peak at ~625 nm indicates the formation of the acetal moiety). Upon completion (~30 min), the reaction was quenched and washed with distilled H_2O in a separatory funnel. The organic phase was extracted with CH_2Cl_2, the organic phase isolated, and reduced to dryness using a rotary evaporator. The residue was then dissolved in dry THF (10 mL), and passed through a plug of Na_2SO_4 and dried using rotary evaporation. Step 2: The round bottom flask containing the dried residue from part 1 was purged with N_2 prior to adding dry THF (10 mL). Under N_2, 3 equiv of TMSOTf (0.022 mL) were added and the solution was stirred for ~90 min at –45°C. Into the reaction mixture, 10 equiv of EtMgCl (2M solution in THF, 0.205 mL) were added at –45°C. The reaction was then stirred for ~4 h at –45°C. In order to avoid an incomplete reaction, the molear equiv of alkyl-Grignard should be double that of TMSOTf in this step. The reaction progress was closely monitored by UV-visible spectroscopy (a small aliquot being treated with drops of 6 M HCl and neutralizing with aq. $NaHCO_3$, the formation of a peak at ~665 nm indicates the formation of the product). Step 3: upon completion, the reaction was quenched with water (1-2 mL), then 6 M HCl (10 mL) was added to the reaction mixture to affect demetalation. The reaction mixture was stirred until the demetalation was complete (as

monitored by UV-visible spectroscopy; formation of a free-base chlorin spectrum upon neutralization indicates the formation of the product). Once demetalation was achieved, the mixture was neutralized with a saturated aq $NaHCO_3$ solution in a separatory funnel. CH_2Cl_2 (10 mL) were added and the organic phase was isolated and dried using rotary evaporator. Product **7a** was isolated by chromatography (silica–60% petroleum ether 30-60/CH_2Cl_2) as a purple solid in 51% (20 mg) yield. MW = 946.8 g/mol; R_f = 0.97 (silica–50% petroleum ether 30-60/CH_2Cl_2); UV-visible ($CHCl_3$) λ_{max} (log ε): 423 (5.15), 516 (3.99), 553 (3.86), 609 (3.82), 666 (4.56) nm; Fl λ_{max} ($CHCl_3$, λ_{exc} = 424 nm): 671, 721 nm, ϕ = 0.29; ^{1}H NMR (300 MHz, $CDCl_3$, δ): 8.41 (d, ^3J = 4.29 Hz, 1H), 8.26 (d, ^3J = 3.40 Hz, 1H), 8.2–7.08 (m, 19H), 7.61 (d, ^3J = 3.60 Hz, 1H), 2.20–2.17(m, 2H), 2.01–1.97 (m, 2H), 0.79 (t, ^3J = 7.18 Hz, 6H), 0.10 (s, 1H), –0.31 (s, 1H) ppm; ^{13}C NMR (100 MHz, $CDCl_3$, δ): 167.4, 158.2, 154.6, 150.7, 145.5, 145.5, 143.6, 143.26, 143.25, 142.98, 142.97, 142.5, 136.9, 134.0, 133.9, 133.71, 133.66, 133.5, 133.2, 130.9, 129.8, 127.7, 125.33, 125.29, 124.34, 124.31, 124.27, 124.1, 124.04, 124.01, 123.8, 123.7, 121.8, 119.8, 108.0, 98.2, 97.7, 34.1, 8.2 ppm; HR–MS (ESI+ of MH^+, 100% CH_3CN, TOF): *m/z* calc'd for $C_{51}H_{35}F_{12}N_4O$: 947.2619, found 947.2603.

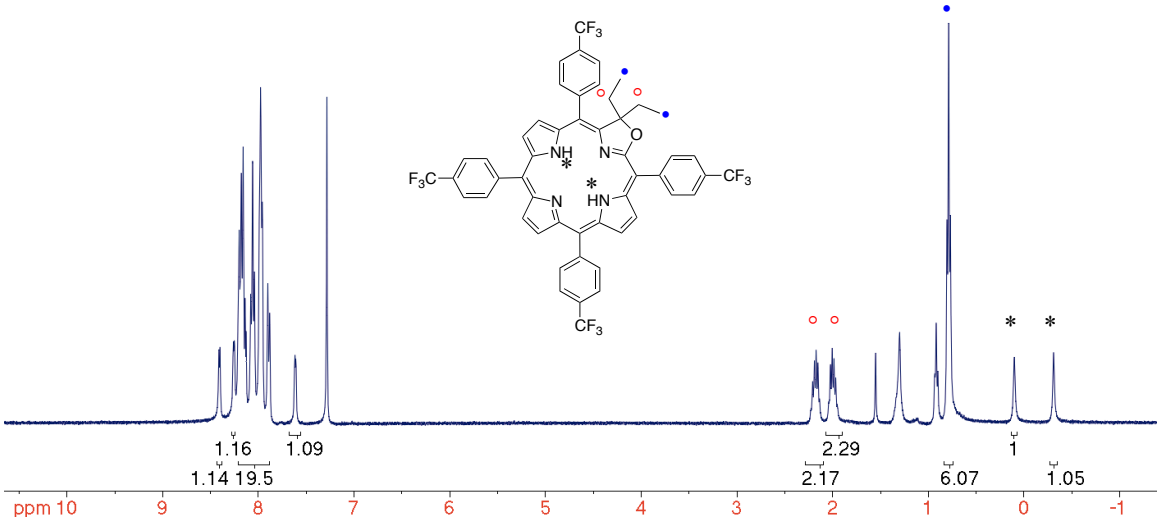

Figure 2-9. Illustrated ^{1}H NMR spectrum (400 MHz, $CDCl_3$) of **7a**.

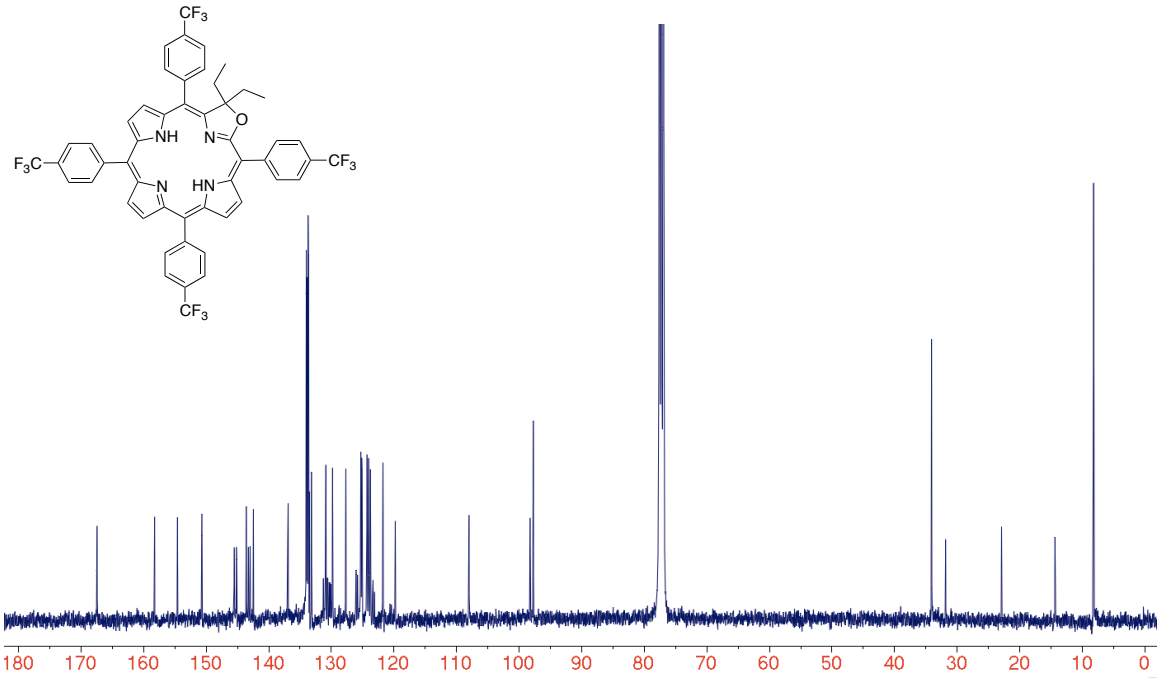

Figure 2-10. ^{13}C NMR spectrum (100 MHz, $CDCl_3$) of **7a**.

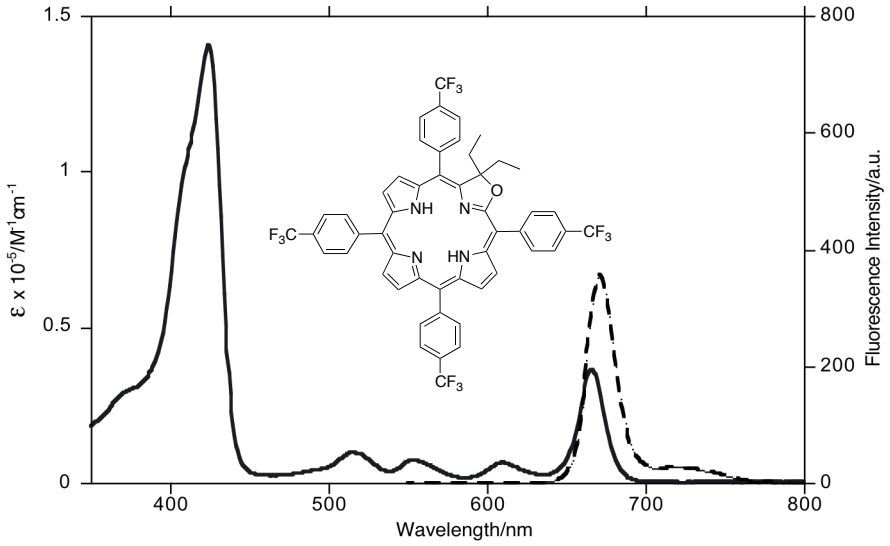

Figure 2-11. UV-vis (solid trace) and fluorescence (broken trace) spectra of **7a** ($CHCl_3$).

***meso*-Tetrakis(4-trifluoromethylphenyl)-3,3-diisopropyl-2-oxachlorin (7b).** Prepared from [*meso*-tetrakis(4-trifluoromethylphenyl)-2-oxa-3-oxo-porphyrinato]Zn(II) (**3Zn**, 53 mg, 5.5×10^{-5} mol) and *i*-PrMgCl according to the reaction procedure described for the preparation of **7a** except for the following: In Part 1, 3 equiv of *i*-PrMgCl (2M solution in THF, 0.083 mL) were added and the solution stirred for ~1 h at –78°C. In Step 2, 3 equiv of TMSOTf (0.03 mL) were added and the reaction was stirred for ~1 h at –78°C. Next, 6 equiv of *i*-PrMgCl (2M solution in THF, 0.164 mL) was added at –78°C, then the reaction was stirred for about ~1 h at this temperature. The product **7b** was isolated by column chromatography (silica–60% petroleum ether 30–60/CH_2Cl_2) as a purple solid in 56% (30 mg) yield. MW = 974.3 g/mol; R_f = 0.97 (silica-50% petroleum ether 30-60/CH_2Cl_2); λ_{max} (log ε): 425 (5.29), 517 (4.11), 554 (3.95), 610 (3.92), 668 (4.67) nm; Fl λ_{max} ($CHCl_3$, λ_{exc} = 425 nm): 673, 718 nm, ϕ = 0.27; ^{1}H NMR (300 MHz, $CDCl_3$, δ): 8.41 (d, ^3J = 4.4 Hz, 1H), 8.22–7.88 (m, 20H), 7.53 (d, ^3J = 2.5 Hz, 1H), 2.55–

2.48 (m, 2H), 1.09 (d, ^{3}J = 6.2 Hz, 6H), 0.67 (d, ^{3}J = 6.6 Hz, 6H), 0.08 (s, 1H), –0.03 (s, 1H) ppm; ^{13}C NMR (100 MHz, $CDCl_3$, δ): 167.5, 161.4, 154.6, 150.5, 145.6, 145.0, 143.9, 143.5, 143.3, 143.0, 136.9, 134.2, 134.0, 133.7, 133.6, 133.4, 133.2, 130.9, 130.7, 129.7, 127.7, 125.3, 125.2, 124.98, 124.95, 124.33, 124.30, 124.0, 123.9, 123.8, 123.7, 122.3, 119.7, 107.9, 101.4, 98.2, 37.0, 19.3, 19.0; HR–MS (ESI+ of MH^+, 100% CH_3CN, TOF): *m/z* calc'd for $C_{53}H_{39}F_{12}N_4O$: 975.2932, found 975.2901.

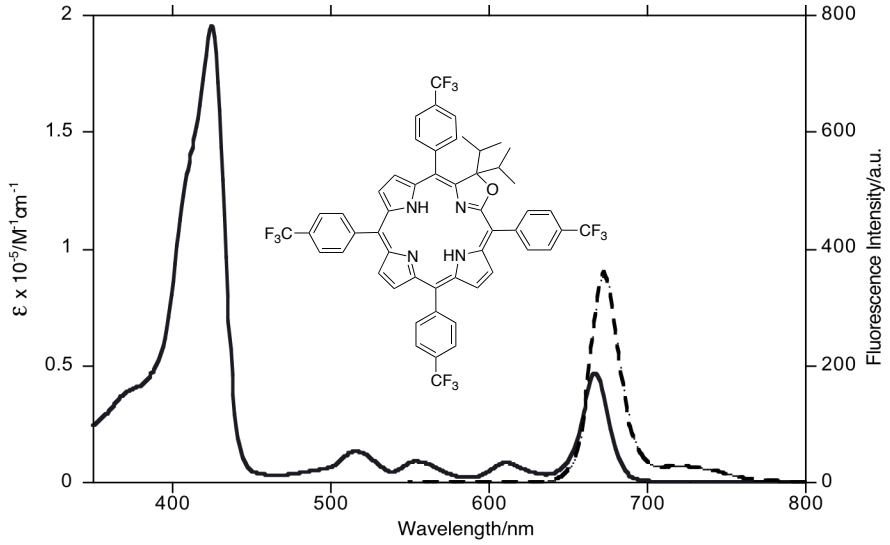

Figure 2-12. UV-vis (solid trace) and fluorescence (broken trace) spectra of **7b** ($CHCl_3$).

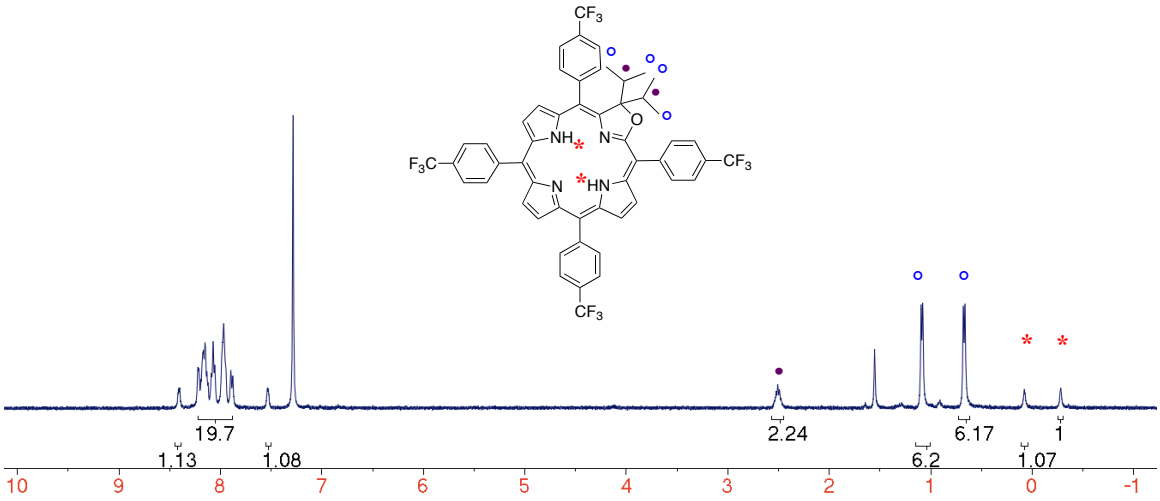

Figure 2-13. Illustrated ^{1}H NMR spectrum (400 MHz, $CDCl_3$) of **7b**.

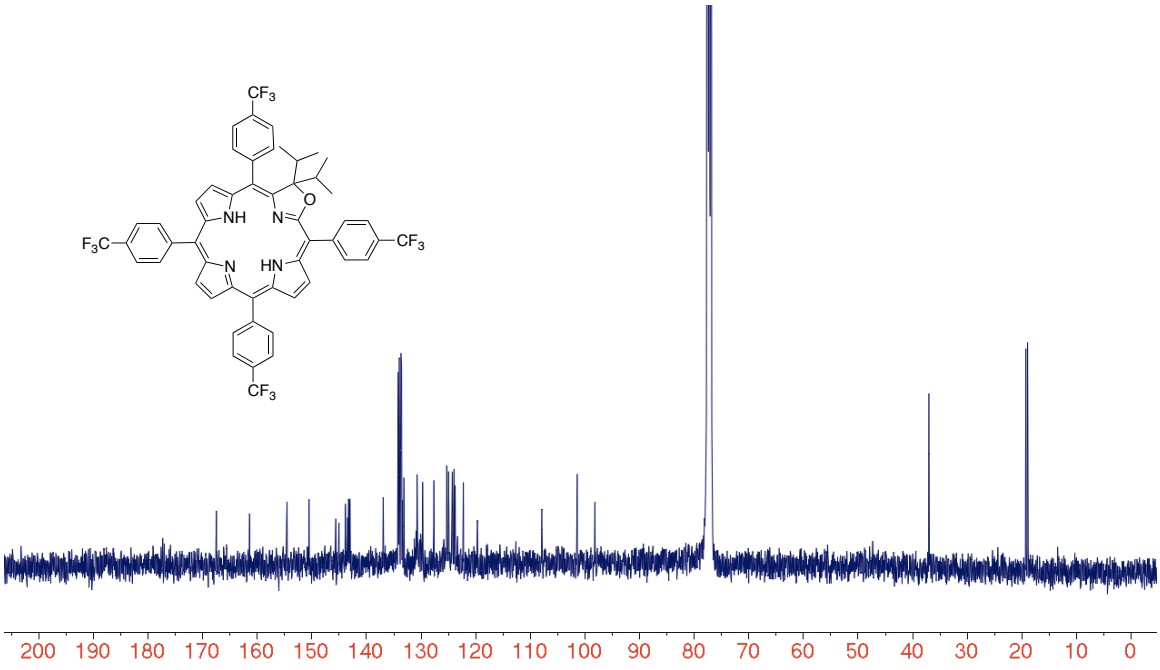

Figure 2-14. ^{13}C NMR spectrum (100 MHz, $CDCl_3$) of **7b**.

2.6 References

1. (a) Akhigbe, J.; Ryppa, C.; Zeller, M.; Brückner, C., *J. Org. Chem.* **2009,** *74* (14), 4927-4933; (b) Brückner, C.; Dolphin, D., *Tetrahedron Lett.* **1995,** *36* (19), 3295-3298; (c) Crossley, M. J.; King, L. G., *J. Chem. Soc., Chem. Commun.* **1984,** (14), 920-922; (d) Gouterman, M.; Hall, R. J.; Khalil, G. E.; Martin, P. C.; Shankland, E. G.; Cerny, R. L., *J. Am. Chem. Soc.* **1989,** *111* (10), 3702-3707; (e) Khalil, G.; Gouterman, M.; Ching, S.; Costin, C.; Coyle, L.; Gouin, S.; Green, E.; Sadilek, M.; Wan, R.; Yearyean, J.; Zelelow, B., *J. Porphyrins Phthalocyanines* **2002,** *6* (2), 135-145; (f) Köpke, T.; Pink, M.; Zaleski, J. M., *Org. Biomol. Chem.* **2006,** *4* (22), 4059-4062.

2. Ogikubo, J., Ph.D. Thesis. *University of Connecticut* **2012**.

3. (a) Zelelow, B. K., G. E.; Phelan, G.; Carlson, B.; Gouterman, M.; Callis, J. B.; Dalton, L. R. , *Sens. Actuators, B* **2003,** *96*, 304-314; (b) Gouterman, M. C., J.; Dalton, L.; Khalil, G.; Mebarki, Y.; Cooper, K. R.; Grenier, M. *Meas. Sci. Technol.* **2004,** *15*, 1986-1994.

4. (a) Khalil, G. E. C., C.; Crafton, J.; Jones, G.; Grenoble, S.; Gouterman, M.; Callis, J. B.; Dalton, L. R., *Sens. Actuators, B* **2004,** *97*, 13-21; (b) Gouterman, M., *J. Chem. Educ.* **1997,** *74*, 697-702; (c) Khalil, G. E. D., P.; Lau, K. S. F.; Imtiaz, S.; King, M.; Gouterman, M.; Sidelev, A.; Puran, N.; Ghandehari, M.; Brückner, C., *Analyst* **2010,** (135), 2125-2131; (d) Brückner, C.; Ogikubo, J.; McCarthy, J. R.; Akhigbe, J.; Hyland, M. A.; Daddario, P.; Worlinsky, J. L.; Zeller, M.; Engle, J. T.; Ziegler, C. J.; Ranaghan, M. J.; Sandberg, M. N.; Birge, R. R., *J. Org. Chem.* **2012,** *77*, 6480–6494; (e) McCarthy, J. R. J., H. A.; Brückner, C., *Org. Lett.* **2003,** *5*, 19-22.

5. (a) Balasubramanian, T.; Strachan, J.-P.; Boyle, P. D.; Lindsey, J. S., *J. Org. Chem.* **2000,** *65* (23), 7919-7929; (b) Strachan, J.-P.; O'Shea, D. F.; Balasubramanian, T.; Lindsey, J. S., *J. Org. Chem.* **2000,** *65* (10), 3160-3172.

3. Expanding Octaethylporphyrin: The Beckmann Rearrangement of Octaethyl-2-oxa-chlorin Oxime

3.1 Introduction

Octaethylporphyrin (OEP) **1** can be converted to a 2-oxochlorin **3** along two pathways: a pinacol-pinacolone rearrangement of the *cis*-vicinal dihydroxy chlorin **2** (Scheme 3-1) and by oxidation of OEP with H_2O_2/H_2SO_4 (piranha solution), presumably as a result of an ß,ß'-epoxidation/epoxide ring opening to generate a *trans*-vicinal dihydroxy chlorin/pinacol-pinacolone rearrangement of the diol sequence.[17-20] The latter reaction was also utilized in a range of regioisomeric diones.[18] Because of the presence of an sp^3-hybridized ß-position, oxochlorin **3** posses a chlorin-type optical spectrum (Figure 3-1). Most importantly, the ketone functionality in oxochlorin **3** was shown to possess regular ketone functionality, and a variety of reactions were reported.[18]

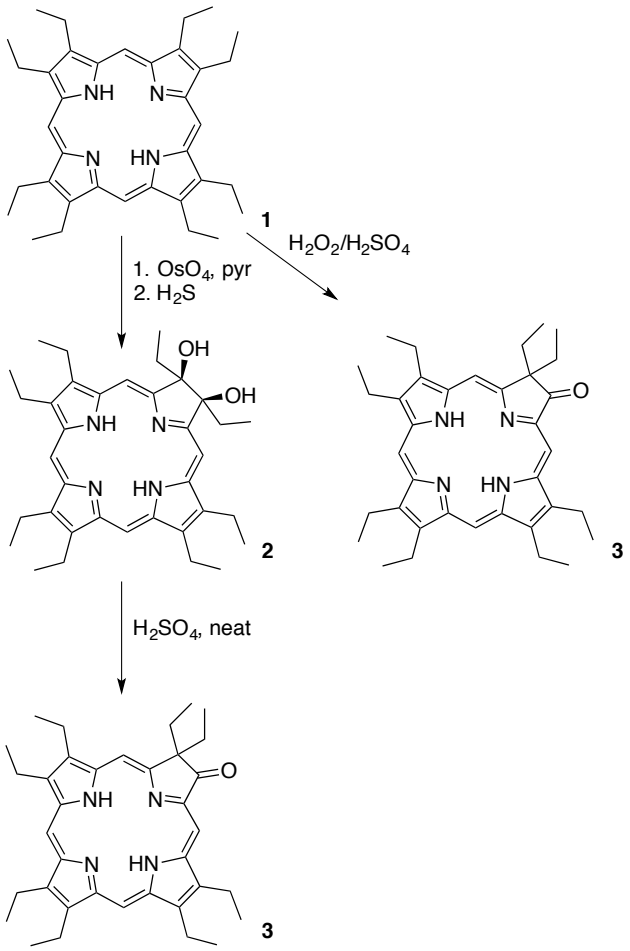

Scheme 3-1. Pathways towards the synthesis of oxochlorin **3**.

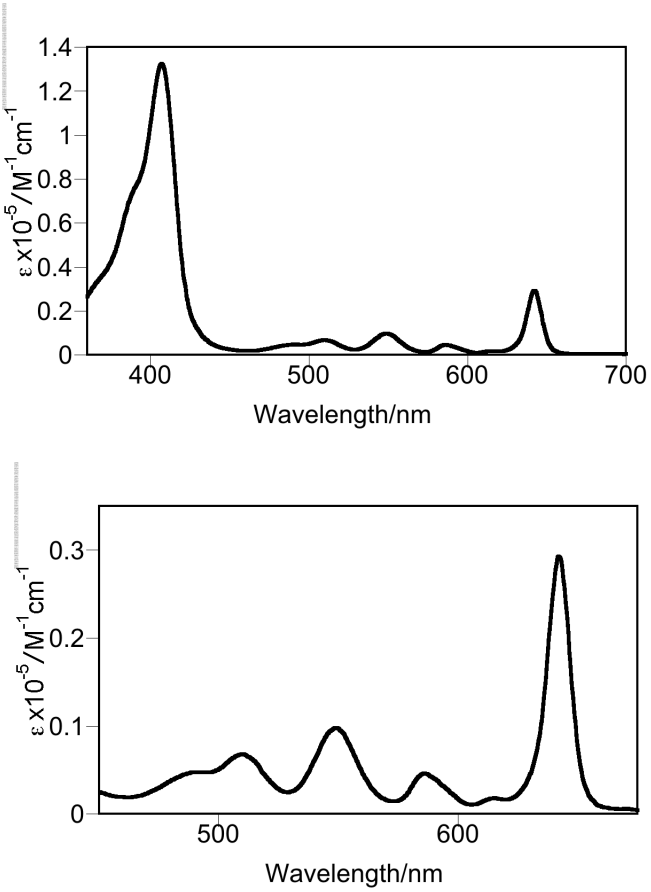

Figure 3-1. UV/Vis spectrum ($CHCl_3$) of oxachlorin **3** (top) and expanded Q-band region of **3** (bottom).

The Beckmann rearrangement is an acid-catalyzed rearrangement of an oxime to an amide. Applied to cyclic oximes, a ring-expansion reaction to form a lactam takes place (Scheme 3-2).[21]

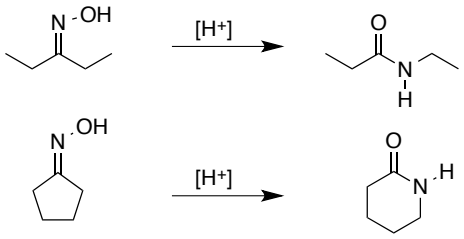

Scheme 3-2. Beckmann rearrangement of linear and cyclic oximes.

If the cyclic oxime is non-symmetric, two possible rearrangements can take place (Scheme 3-3), but generally the product resulting from the migration of the moiety *trans* to the leaving hydroxyl group is observed, suggestive that the 1,2-shift and the N–O cleavage reactions are concerted.[22-24] However, the configuration of the oxime is frequently not known and steric effects may over-ride the stereo-electronic effects, making an outcome of the reaction not always easily predictable. Thus, a literature survey of the reaction shown in Scheme 3-3 reveals that both products are observed depending on the reaction conditions or the presence of substituents on the molecule. [25-29]

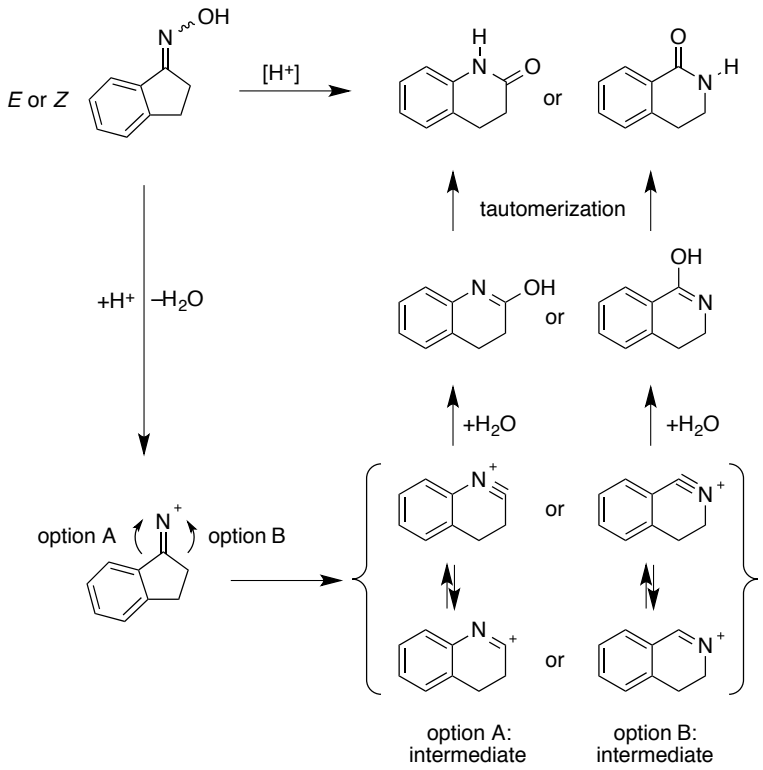

Scheme 3-3. Beckmann rearrangement of cyclic oximes.

The Brückner group is interested in the formal replacement of a pyrrolic subunit in porphyrins by a non-pyyrolic heterocycle (see also Chapter 1.4).[30] In due course of this work, they demonstrated the step-wise expansion of a free base octaethylporphyrin to

incorporate a pyridinone moiety, utilizing an aldol condensation as the key step (Scheme 3-4).[1] This reaction was previously shown for the corresponding Nickel(II) complex.[31] This serves as a precedent that octaethylporphyrin is amenable to expansion reactions. In fact, the group showed that the reaction can be performed twice on the same molecule, resulting in a bis-expanded system.[1]

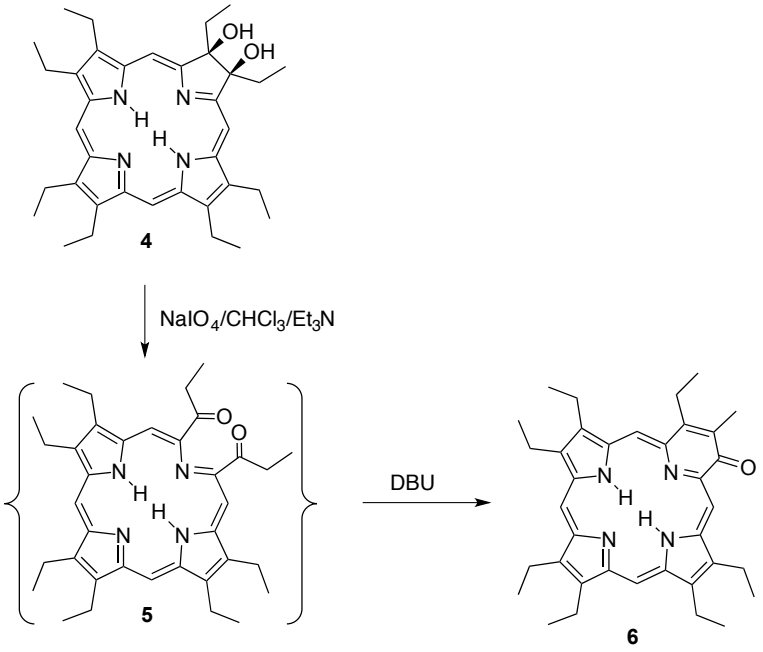

Scheme 3-4. Expansion of octaethylporphyrin via an aldol condensation reaction of the intermediate secochlorin bisketone **5**.[1]

The Brückner group also showed a Beckmann reaction of a *meso*-arylporphyrin ß-oxime **8** resulted in the expansion of the porphyrin (Scheme 3-5).[32] Thus, an α-oxo oxime was rearranged and the pyrrolic moiety expanded to a pyrazinoporphyrin imide moiety in **9**. The reaction shows an intriguing counter-intuitive regio-selectivity. Oxime **8** is present in the H-bonded configuration shown (known by NMR spectroscopy and a solid state structure of the compound). Yet, the expected stere-oelectronic product **13** is

not formed. Instead, the imide **9** is the exclusive product. This reaction highlights that the particular steric and likely also electronic restrictions posed by the porphyrin framework will not allow easy predictions.

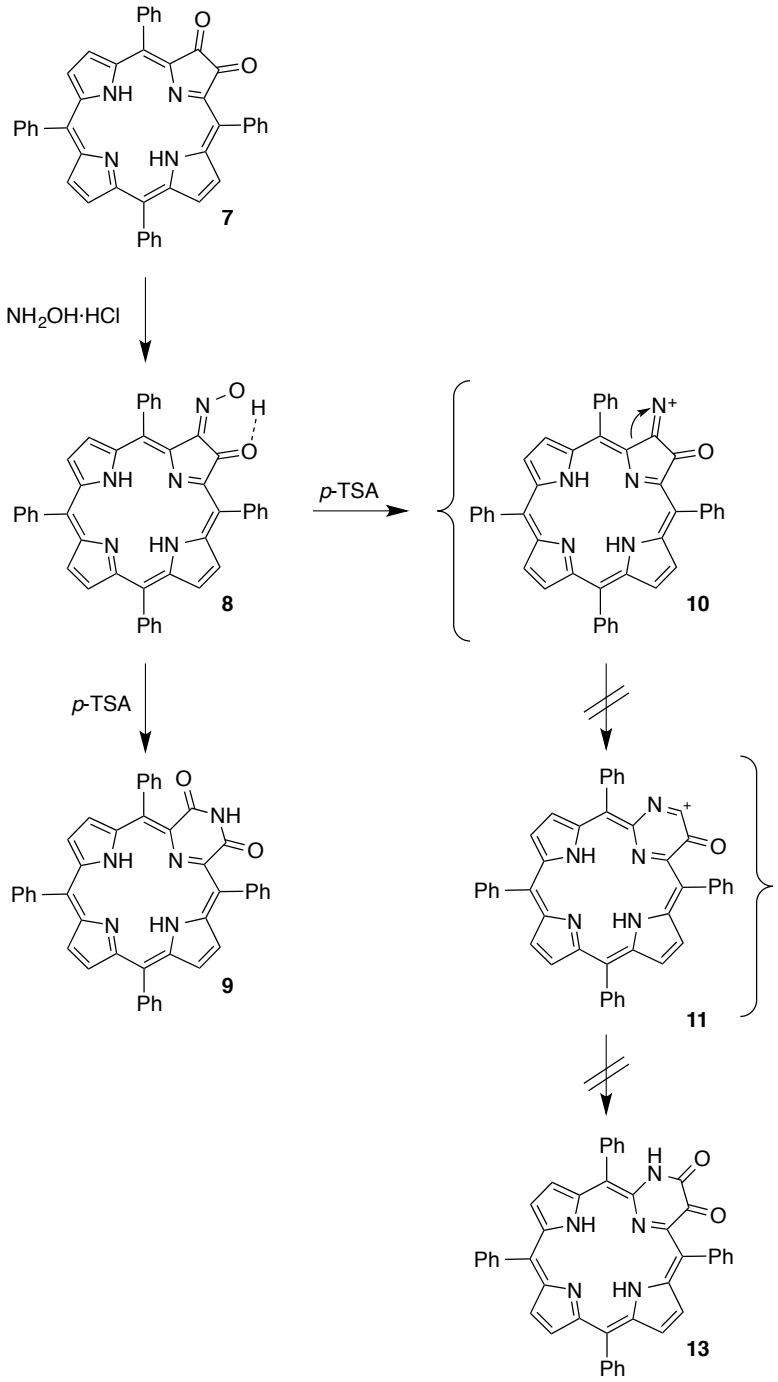

Scheme 3-5. Observed and expected Beckmann product of oxime **8**.

This chapter will describe the results obtained when we converted the well-known oxochlorin **3** to its oxime and submitted it to Beckmann rearrangement conditions. The planned synthesis is shown in Scheme 3-6. We expect the formation of the oxime to be smooth. However, a firm prediction as to which of the two possible diazine-based pyrrole-modified porphyrins could be expected to be the outcome of the Beckmann reaction cannot be made (for a further discussion, see below).

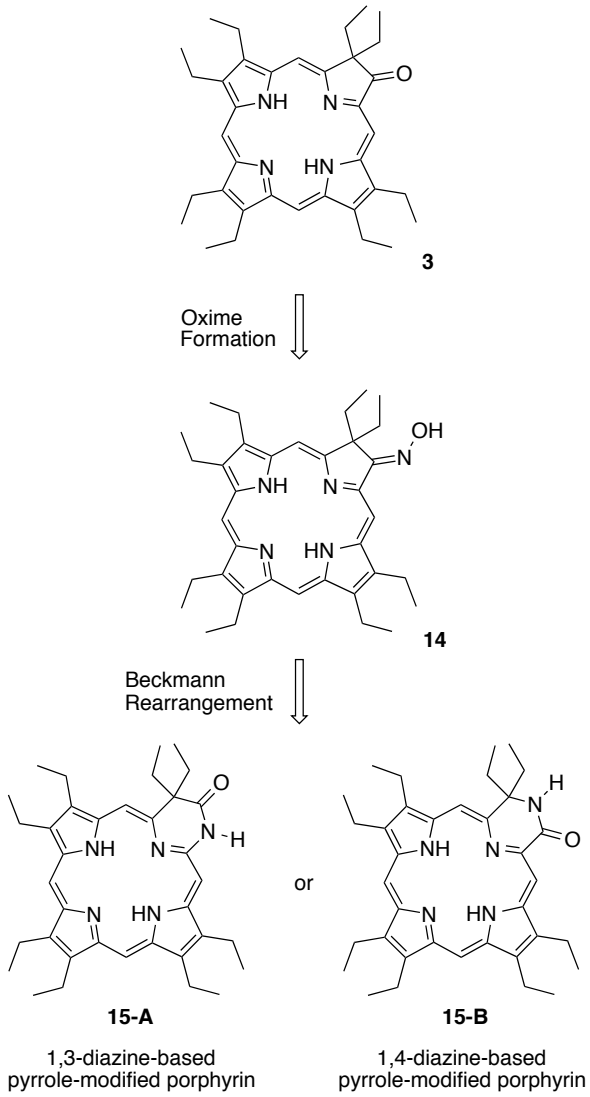

Scheme 3-6. Planned synthesis of pyrazinoporphyrin **13**.

3.2 Results and Discussion

3.2.1 Oximation of Octaethylporphyrin β-oxochlorin

The properties of β-oxoporphyrin **3** and its metal complexes were studied.[19,33,34] The oximation of the closely related etioporphryin-based oxochlorin was mentioned in a report,[33] but scant details were disclosed; the oximation of the octaethyloxochlorin was not reported. Its oximation proved straightforward.

Oxochlorin **3**, prepared along the diol-pinacol-pinacolone rearrangement route (Scheme 3-7),[19,20] did not react with a very large (~100-fold) molar excess of hydroxylamine at room temperature (as the dione **7** reportedly reacted at).[32] Increasing the reaction temperature, however, resulted in the formation of a product in good yields (Scheme 3-7). The expected composition of the product **14** ($C_{36}H_{47}N_5O \cdot H^+$, MH^+) was confirmed by the exact mass by ESI(+) HR-MS. Characteristic signals for the imine functionality was seen in its ^{13}C NMR spectra (164.9 ppm). Further, in the ^1H NMR spectrum, a diagnostic and D_2O-exchangeable signal at 8.06 ppm is assigned to the hydroxyl group of the oxime. Notably, the appearance of diastereotopically split methylene protons signals around 2.71–3.54 ppm in the ^1H NMR spectrum marks the presence of the new hydroxylamine group. The presence of diastereotopically split methylene proton signals was not present in the ^1H NMR spectrum of **3**.

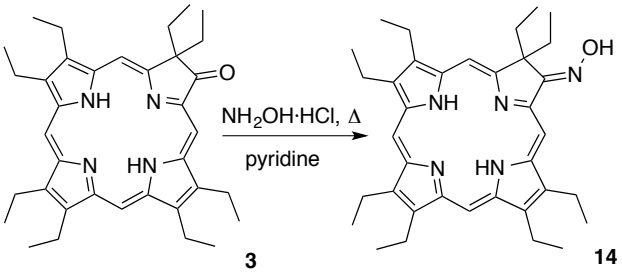

Scheme 3-7. Synthesis of OEP oxime **14**.

Moreover, the UV-vis spectrum of **14** is chlorin-like, compared to the spectrum of the oxochlorin **3**, with a slightly blue-shifted Soret band and a slightly red-shifted λ_{max} value (see Figure 3-2). Interestingly, **14** possess a higher fluorescence emission yield compared to that of the parent compound **3**. ($\phi = 0.14$ for **3**; $\phi = 0.18$ for **14**)

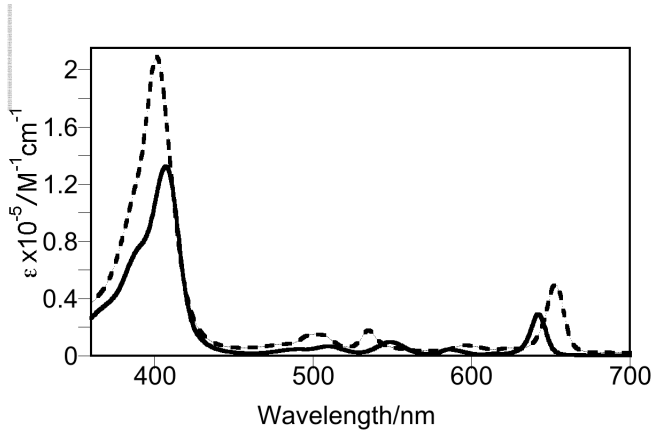

Figure 3-2. UV-vis spectra ($CHCl_3$) of oxochlorin **3** (solid trace) and its corresponding oxime **14** (broken trace).

3.2.2 Beckmann Rearrangement of Octaethylporphyrin Oxime

With the oxime **14** in hand, we could attempt an acid-induced Beckmann rearrangement. Many different acids have been described as suitable to induce this reaction.[22,23] The results of the screening of a number of acids are shown in Table 3-1.

Most acids did not result in any reaction (as determined by the observation of the oxime **14** by TLC). However, PCl_5 under anhydrous conditions at ice bath temperatures was found to lead to a reaction.[35]

Acid	Result
TsCl	No rxn
p-TSA	No rxn
$SOCl_2$	No rxn
TFA	No rxn
H_2SO_4	No rxn
HCl	No rxn
PCl_5	**Reaction**

Dual Acid System	Result
PCl_5 + $SnCl_4$	Rxn
PCl_5 +$SnCl_4$·$5H_2O$	Rxn
PCl_5 + $InCl_3$	Rxn
PCl_5 + TMSOTf	Rxn
PCl_5 + Ti-^{i}OPr	Rxn
PCl_5 + BF_3·OEt_2	**Rxn**

Table 3-1. Acids screened to inducing a Beckmann rearrangement of **14**.

The reaction of **14** with PCl_5 lead to the formation of several products, one such product having higher polarity and a different blue color from the dark purple-brown oxime **14**. An aqueous workup of the reaction mixture followed by extraction with methylene chloride, rotary evaporation to remove solvent and chromatographic separation of the reaction products led to the isolation of **14**. A LRMS ESI(+) spectrum of the first product isolated was found to possess a mass/charge ratio of 566.5 *m/z*, as expected for the desired Beckmann product. After this discovery, and in an attempt to improve the conversion of the **14** to the new product for characterization, a dual Lewis acid system was investigated. The use of a dual Lewis acid system involving PCl_5 and BF_3·OEt_2 proved to improve conversion of the starting material and formation of the major product, **17** (Scheme 3-8).

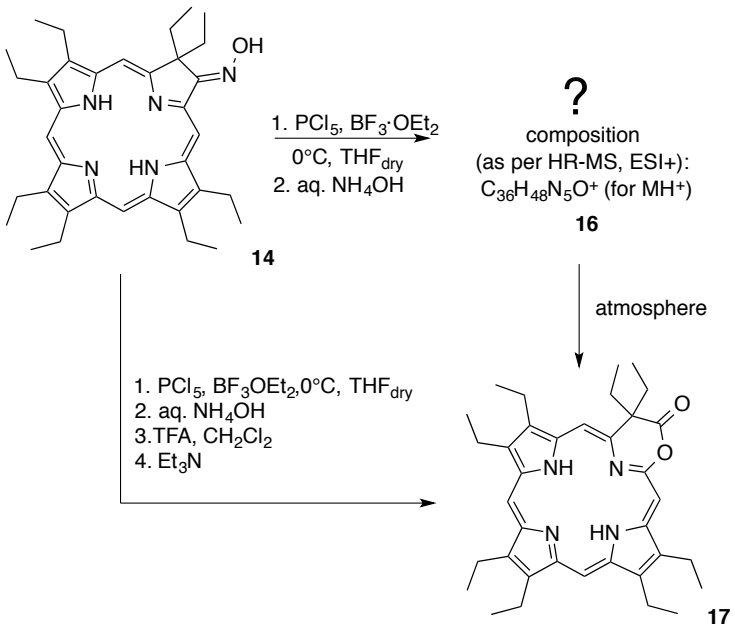

Scheme 3-8. Intermediate and final product result of **the acid-**induced rearrangement of **oxochlorin oxime 14**.

Upon workup we found that the initially formed **16** was rather unstable, and spectroscopic analyses provided contradictions as to what would be expected if the structure were a Beckmann rearranged product **15**. Spectroscopic analysis shows that product **16** is different from reactant **14**, but is still a constitutional isomer; their mass and composition are identical (expected for $C_{36}H_{47}N_5O$, 566.3846 as per HRMS ESI(+). The product compound is, unlike oxime **14**, only weakly fluorescent but still exhibits a chlorin like UV-spectrum, with clearly defined Q-bands (Figure 3-3, 3-4). The Soret band of **16** is significantly blue-shifted compared to both the oxochlorin **3** and its oxime **14**, and some of its Q-bands shifted positions.

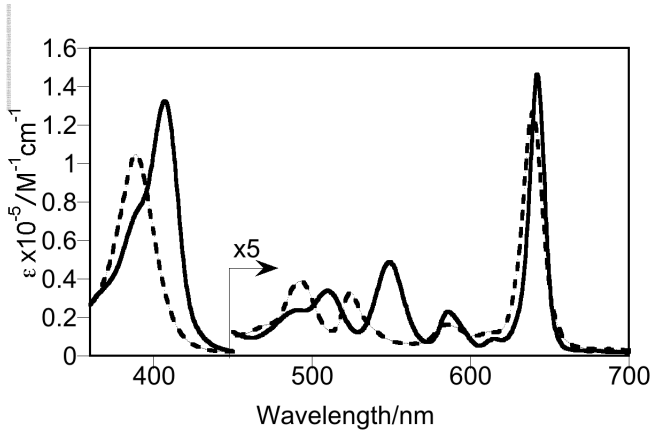

Figure 3-3. UV/Vis spectra ($CHCl_3$) of oxochlorin **3** (solid trace) and product **16** (broken trace).

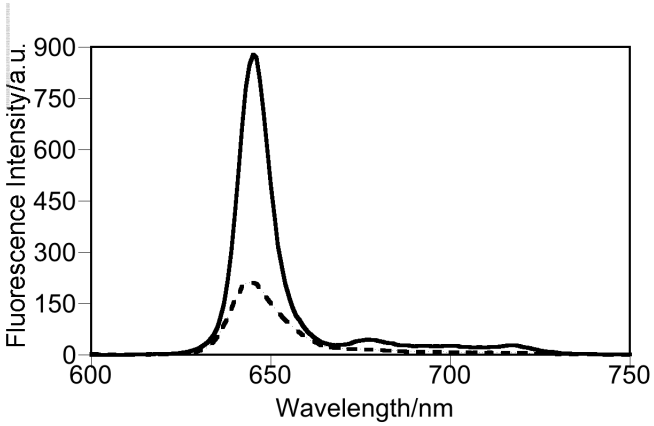

Figure 3-4. Fluorescence spectra (C_6H_6) of oxochlorin **3** (solid trace) and product **16** (broken trace).

The two possible outcomes of a Beckmann rearrangement of **14** are shown in Scheme 3-9. Depending on which of the residues undergoes a 1,2-shift, either the 1,3- or a 1,4-diazine-based system is formed. Arguments can be brought forward for either options: the shift of the residue *anti* to the leaving group is the stereo-electronically preferred version while the shift *cis* to the leaving group was shown to be preferred in the

precedent case illustrate above (Scheme 3-5).[32] Also, on the basis of all atoms possessing electron octets, the presumed most prevalent resonance structure of the intermediate cation is shown in bold. In case of the *cis*-elimination this cation is in a benzylic position and thus much more stabilized that the *trans*-reaction product cation.

The mass and composition of product **16** as per HRMS ESI(+) appeared to be indicative of the presence of the Beckmann rearranged product of **14**. The presence of shifted meso and diastereotopic protons in the ^{1}H NMR spectrum, as well as shifts in the UV-vis spectrum, coupled with a decrease in the quantum yield of **16** from that of **14**, seemed to further the support for the structure of **16** as the Beckmann rearranged product (Figure 3-5). However, the ^{1}H and ^{13}C NMR provide contradictory information for the assignment of the proposed structure of **16** (Figure 3-6). Primarily, there is no presence of an N-H proton in the ^{1}H NMR spectrum. While there are shifts in the meso protons, as well as in the diastereotopic protons of the ^{1}H NMR spectrum, there is also the presence of a carbonyl ketone carbon peak in the ^{13}C NMR spectrum, and no diagnostic peak shown for that of the proposed structure of **16**.

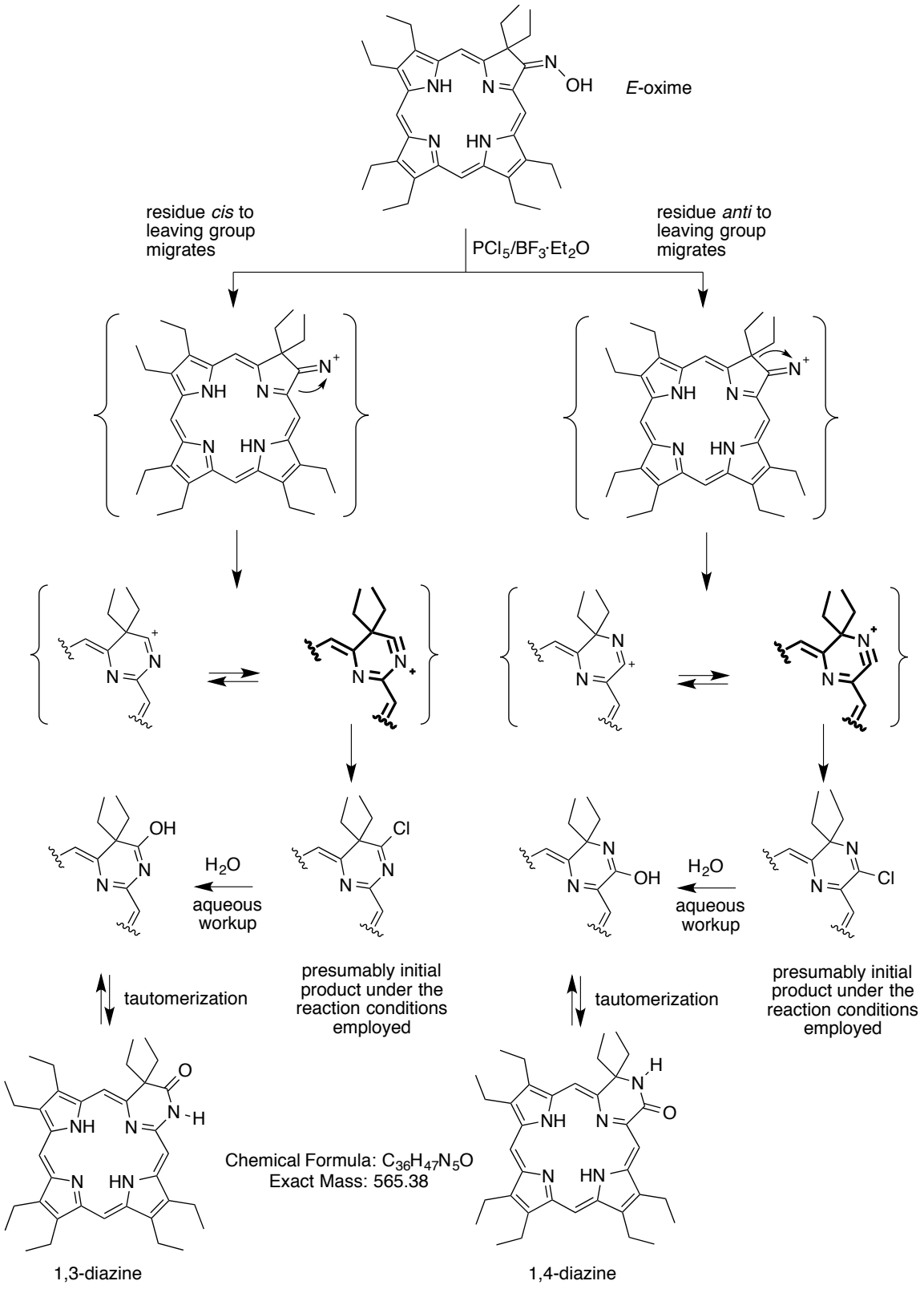

Scheme 3-9. Possible outcomes of a Beckmann rearrangement of **14**.

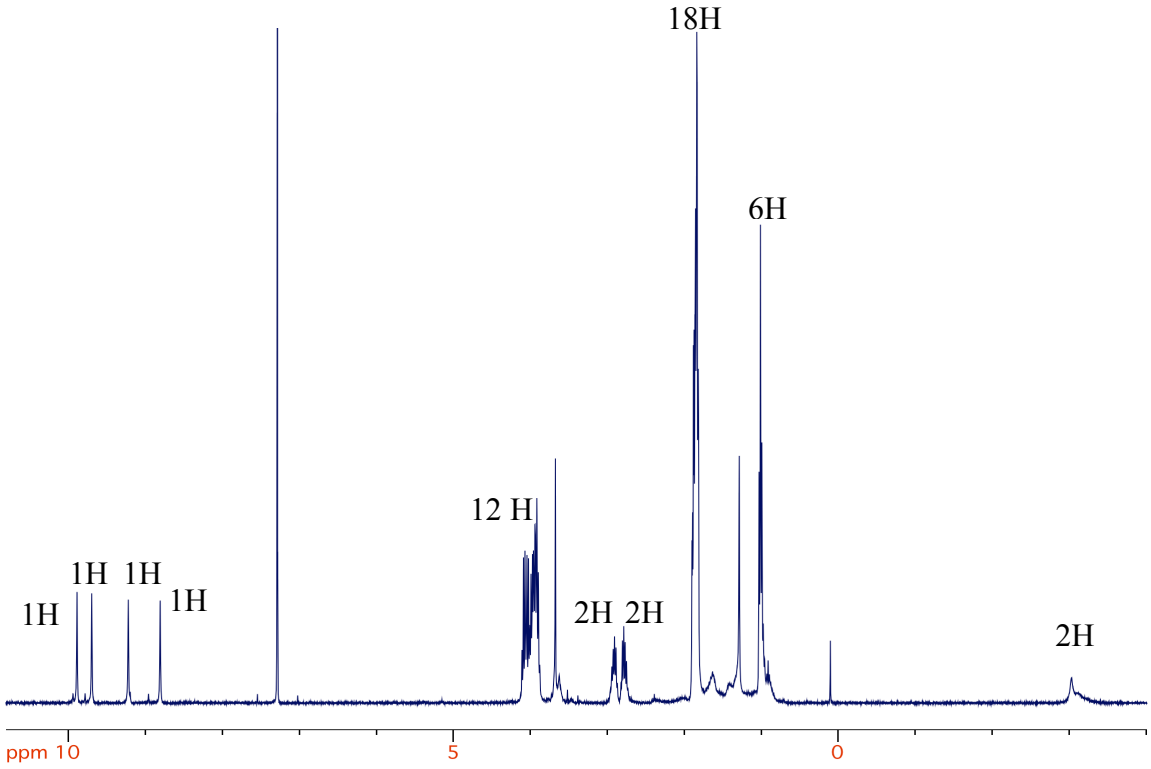

Figure 3-5. ^{1}H NMR ($CDCl_3$, 400 MHz) spectrum of **16**.

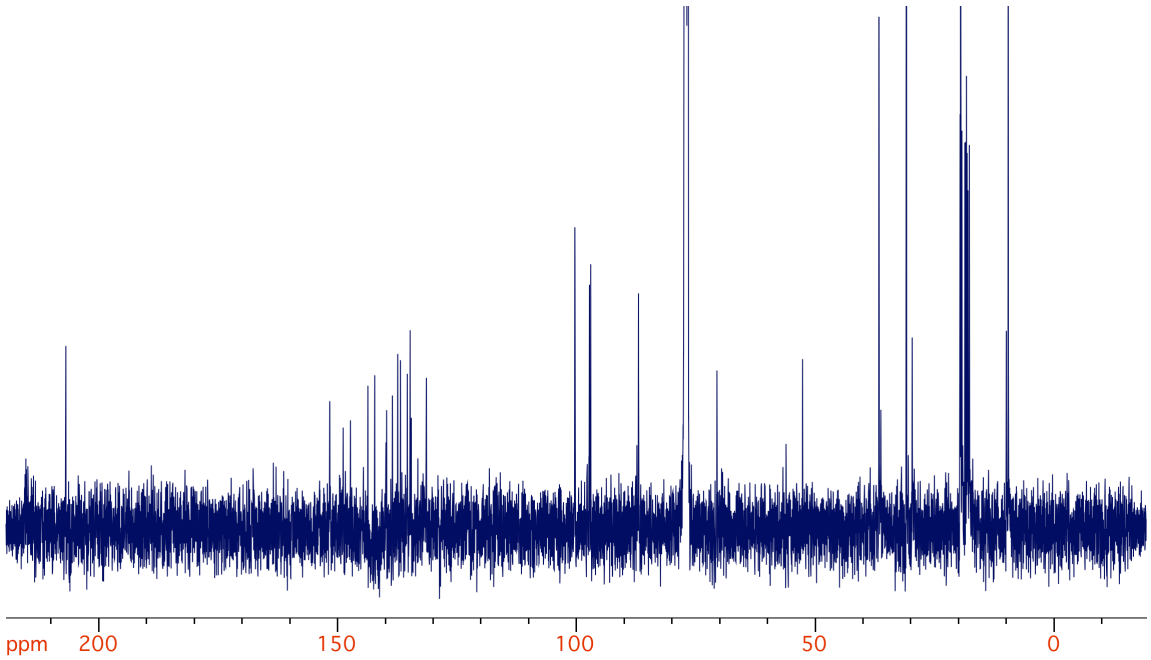

Figure 3-6. ^{13}C NMR ($CDCl_3$, 100 MHz) spectrum of **16**.

Tandem mass spectrometry was utilized to investigate the reactivity of this pyrrole-modified porphyrin (in the gas phase). Collision-induced fragmentation spectra were shown by the Brückner group to be particularly useful for the characterization of pyrrole-modified porphyrins.[36] In unmodified porphyrins, the collision-induced fragmentation spectra are dominated by fragmentations of the porphyrin substituents. In pyrrole-modified porphyrins, the weakened modified pyrrole moieties break apart first, giving rise to diagnostic fragments.

The MS^2 spectrum of the Beckmann product **16** is shown (Figure 3-7). The well-defined fragmentations do not appear to be a straightforward indication of the presence of the lactam-moiety (Figure 3-7). The loss of a fragment of a mass of 30 amu could potentially indicate the loss of a CH_2NH_2 group. The fragments of 59, 74, 89 and 103 amu could possibly be indicative of a loss of different forms of an ester group, which does not support the fragmentation pattern that would be expected for the fragmentation of a lactam-moiety. There is no observed loss of a carbonyl or amide functionality. The fragmentation patterns seem to contradict the presence of a lactam-moiety.

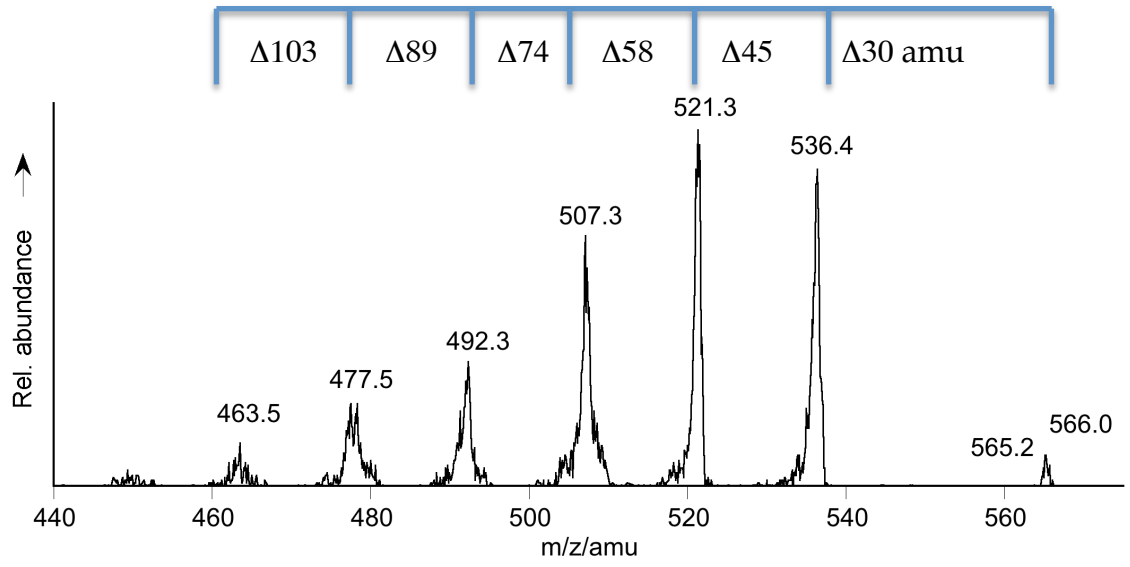

Figure 3-7. Collision-induced fragmentation spectrum of the *m/z* species 566, the major Beckmann product.

Another major issue contradicting both proposed lactam structures for **16** is the finding detailed below, namely the fact that they readily decompose (particularly under acidic conditions) to form the lactone **17**. The connectivity of this compound was proven by single crystal crystallography (Figure 3-13). The facile conversion of a lactam to a lactone seems unlikely as most generally, the reverse reaction is much more preferred.

3.2.3 Conversion of the Primary Beckmann Product to 1-Oxa-4-azacyclohexene-based Pyrrole-modified Porphyrin (17)

The primary Beckmann product **16** converted readily upon workup to a novel compound **17**, of the composition $C_{36}H_{46}N_4O_2$ (as per HR-MS ESI+), suggestive that a hydrolytic event had taken place. Treatment of crude **16** with TFA during the workup procedures converted **16** completely to the novel compound **17**, in up to 24% overall isolated yield.

The UV-vis spectrum of **17** is nearly identical to that of **16**, but exhibits a slight blue shift relative to that of **3** (Figure 3-9). Compound **17** possesses a higher fluorescence yield ($\phi = 0.09$) than **16** ($\phi = 0.05$) but less so than both **14** ($\phi = 0.18$) and **3** ($\phi = 0.14$) (Figure 3-10).

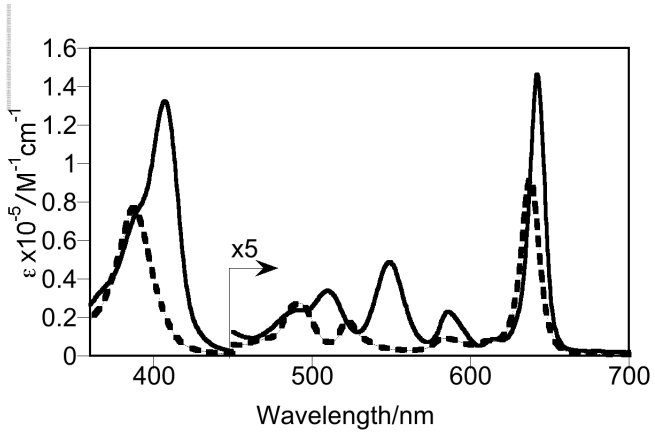

Figure 3-8. UV/Vis spectra ($CHCl_3$) of oxochlorin **3** (solid trace) and product **17** (broken trace).

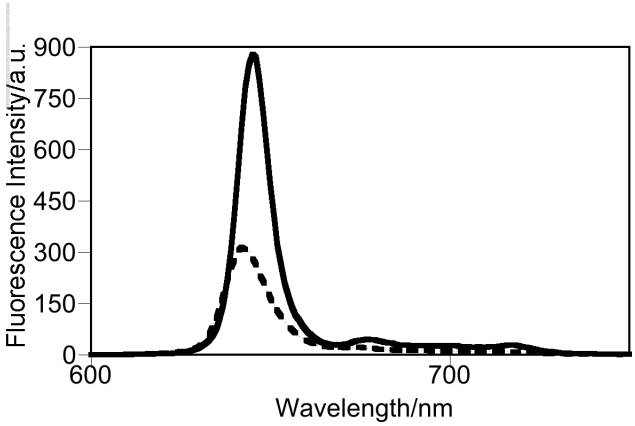

Figure 3-9. Fluorescence spectra (C_6H_6) of oxochlorin **3** (solid trace) and product **17** (broken trace).

The ^{1}H NMR spectrum of compound **17** is shown in Figure 3-11. It shows the signals for a compound of the same low symmetry as the unknown compound **16** and the oxime starting material, **14**, as indicated by the presence of four signals that can be assigned to the *meso*-protons (singlets at 9.94, 9.78, 9.20, and 8.96 ppm, 1H each). It further reveals the presence of shifted diastereotopic methylene protons compared to the spectrum of **16** in which two protons are shifted downfield around 2.96 ppm and two are shifted upfield to around 2.72 ppm (Figure 3-11). The ^{13}C NMR spectrum of **17** has a diagnostic signal for the carbonyl carbon of the lactone moiety at 172.9 ppm (Figure 3-12).

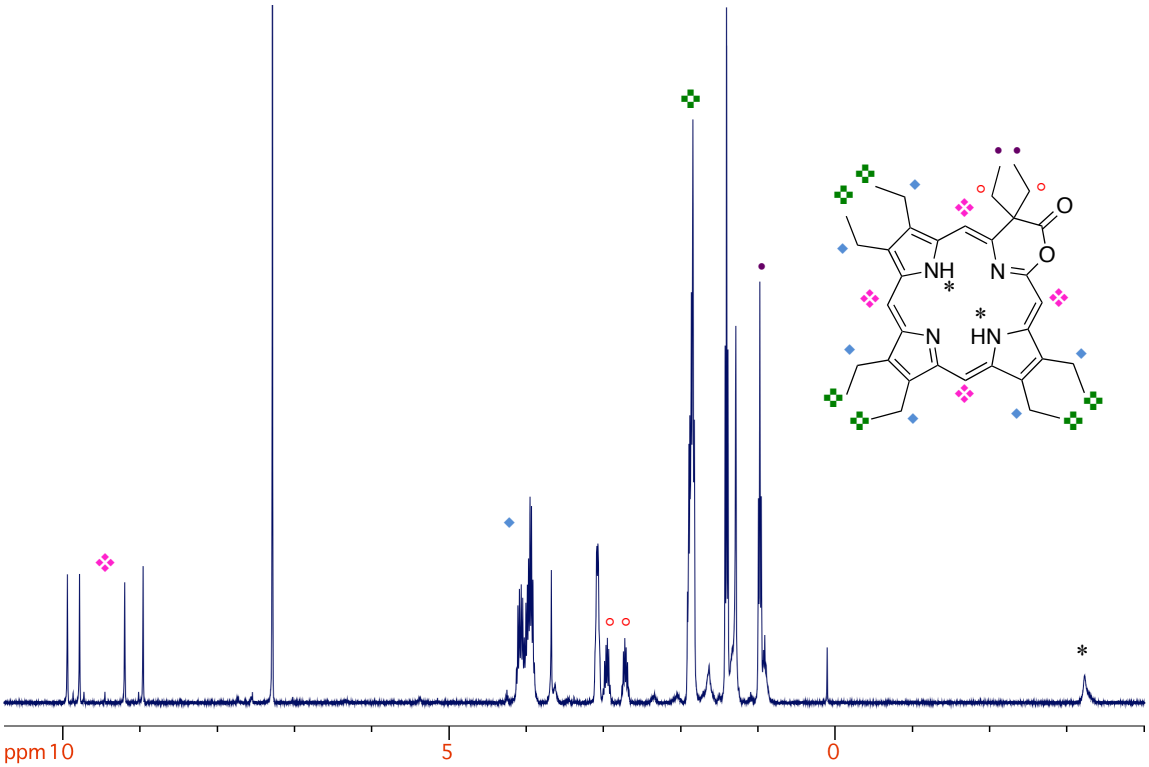

Figure 3-10. Illustrated ^{1}H NMR ($CDCl_3$, 400 MHz) spectrum of product **17**.

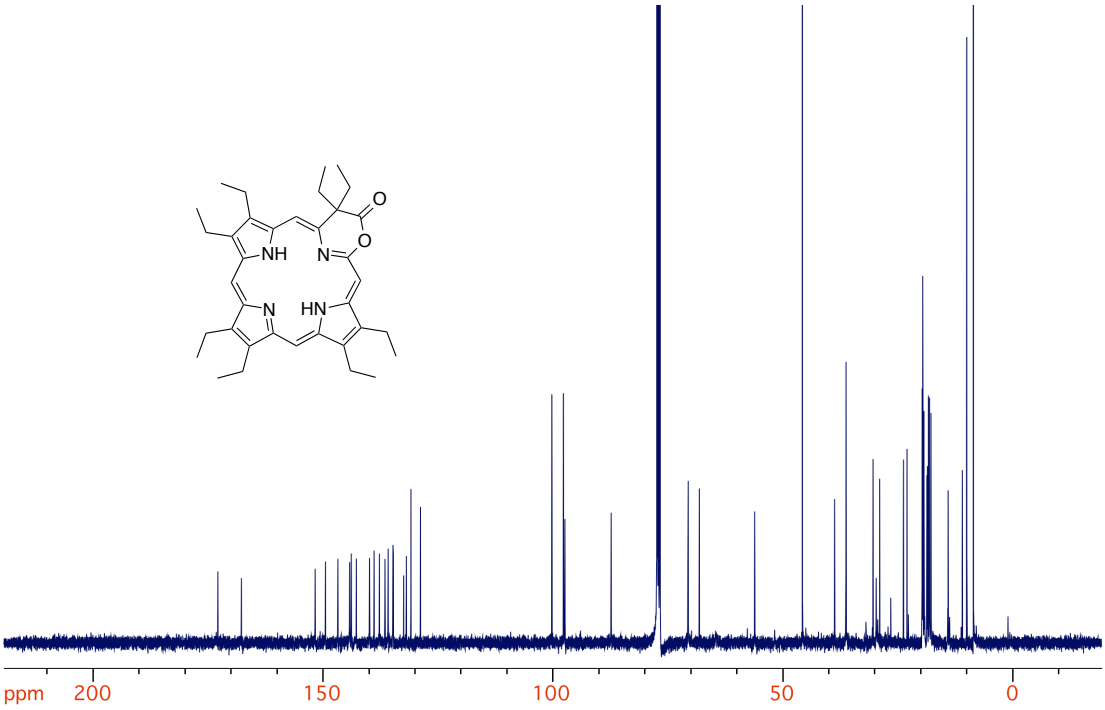

Figure 3-11. ^{13}C NMR ($CDCl_3$, 100 MHz) spectrum of product 17.

One in our group, Ruoshi Li, was fortunate enough to be able to grow a crystal suitable for single crystal diffraction analysis. The result is shown in Figure 3-13. The compound proved indeed to be a lactone. It possesses no precedent among pyrrole-modified porphyrins. The crystal structure reveals that the molecule is mostly planar, with slight distortion of the pyrrole-modified ring around the lactone-moiety. The crystal structure revealed the preference of the formation of the isomer where the carbonyl group is adjacent to the geminal ethyl substituents. This further explains the presence of diastereotopic protons in the ^{1}H NMR spectrum as the ethyl substituents are oriented above and below the plane of the porphyrin ring due to their hindered rotation due to their proximity near the carbonyl carbon.

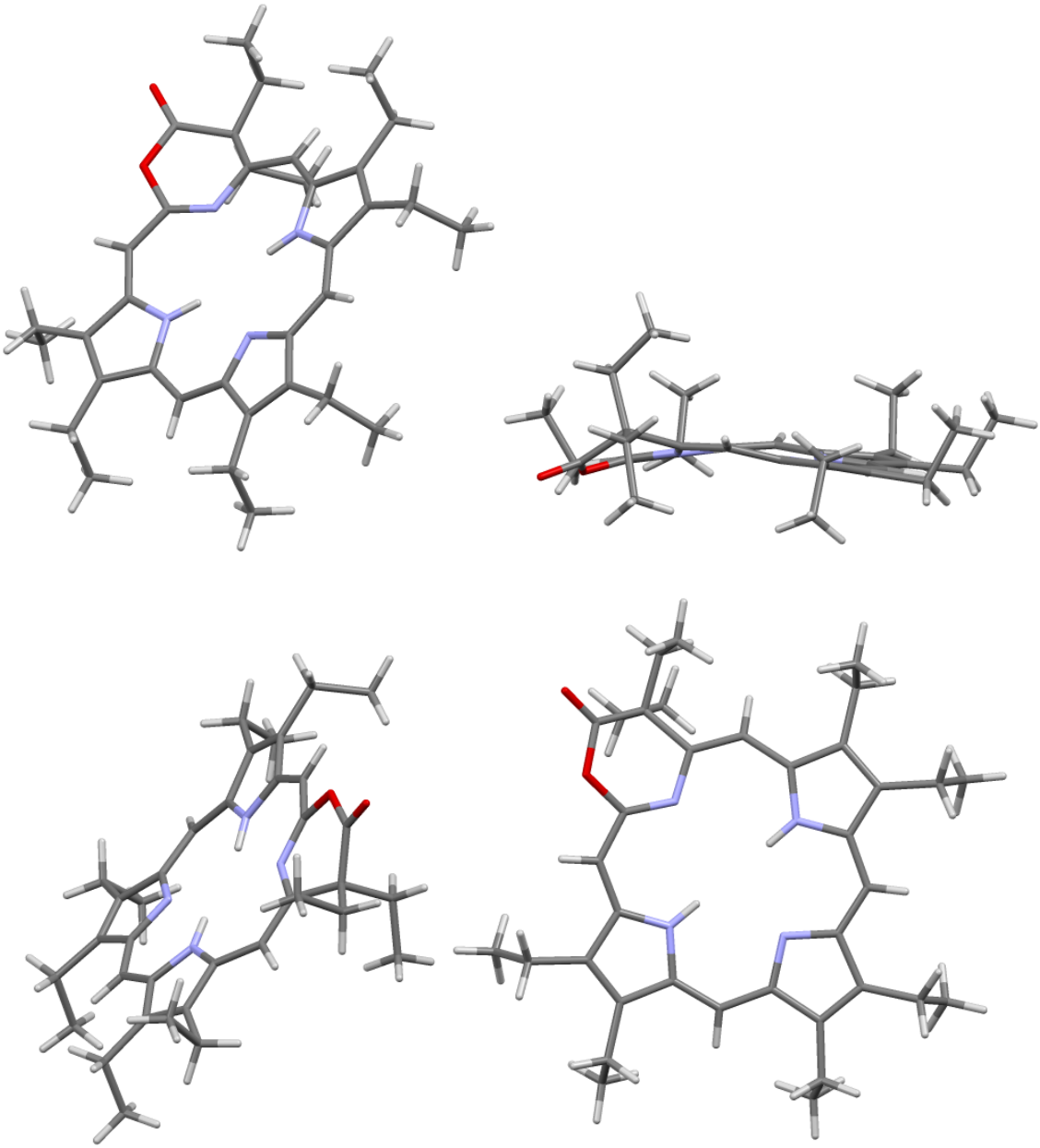

Figure 3-12. Stick model of the single crystal X-ray structure of product **17**. All disorder and solvent molecules omitted for clarity. Structure solved by M. Zeller, Youngstown State University, Youngtown, OH.

To gain further insight into the reactivity of **17**, particularly with respect to a direct comparison to that of its precursor **16**, a collision-induced fragmentation spectrum was run (Figure 3-14).

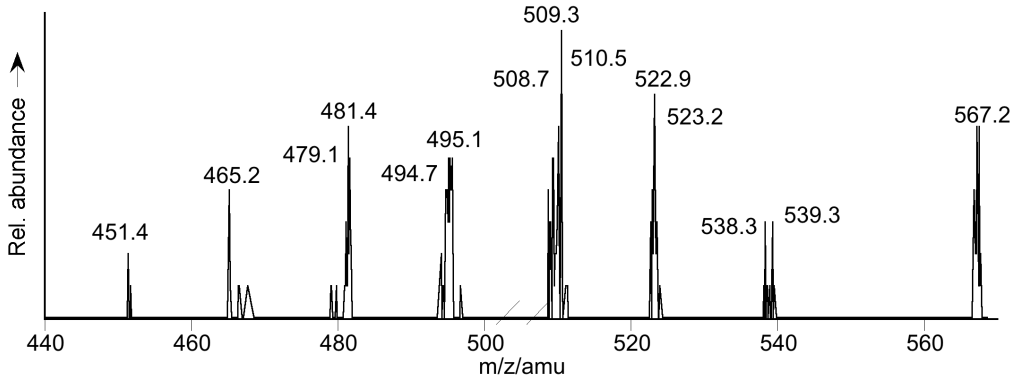

Figure 3-13. Tandem mass spectrum, collision induced dissociation of product **17**.

The lactone structure and the presence of the ß-ethyl groups explain the majority of the fragmentations. Shown in Scheme 3–10 we present a proposed fragmentation scheme, rationalizing all mass peaks observed. All ethyl substituent fragmentations observed were described previously for other ß-ethylporphyrins.[37,38] The fragmentations of the lactone moiety (loss of O, CO, or CO_2) are consistent with the expected fragmentation of lactones in general, and that of porpholactones in particular.[36] It is important to know that we have no genealogical information about the fragments.

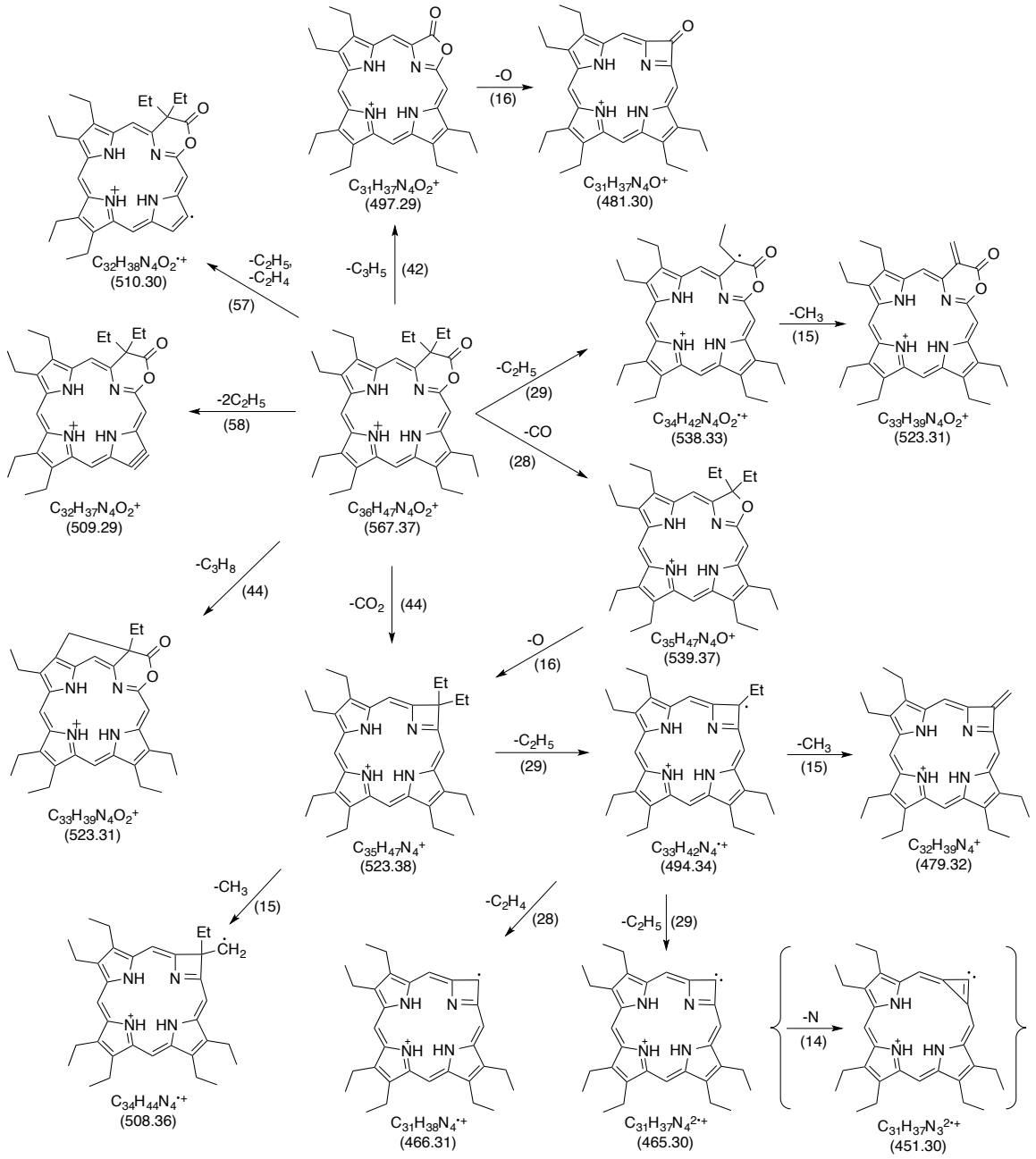

Scheme 3-10. Rationalization of the collision induced dissociation mass spectrum of product **17** (ESI+).

3.3 Conclusion

The addition of hydroxylamine hydrochloride to octaethyl β-oxochlorin derivative **3** led to the formation of the expected oxime. In an attempt to affect the Beckmann rearranged product of this oxime, it was reacted under typical Beckmann conditions (super-stoichiometic amounts of PCl_5 and $BF_3 \cdot OEt_2$). The initial product formed could not be identified but it further hydrolyzed to a 1,3-oxazin-4-one-based pyrrole-modified porphyrin **17**. Considering the structure of **17**, we can safely eliminate the proposed structure **16** (the 1,4-diazastructure) for the initial Beckmann rearrangement product since the hydrolytic conditions that interconvert these two are highly unlikely leading to (more) framework rearrangements. Does this make the 1,3-diaza structure for **16** more likely? We also believe this is not the case as it would seem highly unlikely for **16**, a structure that is resonance stabilized, to hydrolize to form **17**, a structure that is not resonance stabilized.

It is tempting to propose the imine structure shown below as the structure of **16**. This would be consistent with the NMR data presented, the composition and the observed hydrolysis to **17**. However, the mechanism of formation of this product is obscure, and certainly not due to a Beckmann reaction.

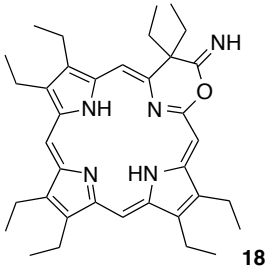

18

Thus, the exact nature of the initial Beckmann rearrangement product remains unclear. Experiments are currently ongoing that aim at the crystallization of this product

so to be able to elucidate its structure using single crystal diffractometry. These crystallizations are made difficult by the hydrolytic instability of this product.

3.4 Experimental Section

3.4.1 Instruments and Materials

2-Oxochlorin was synthesized as reported in literature.[18,19] Preparative (20 × 20 cm, glass-backed, silica gel 60, 500 or 1000 μm thickness) TLC plates and flash column silica gel (premium grade 60, 32–63 μm, SorbTech, Atlanta, GA, U.S.A.) were used for the chromatographic separations and analyses of the products. Flash column chromatography was performed manually in glass columns on normal-phase silica (solvents used are indicated; isochratic elution modes). The fluorescence quantum yields (ϕ) were determined relative to those of octaethylporphyrin (ϕ = 0.13 in benzene)[39]; $\lambda_{excitiation} = \lambda_{Soret}$.

3.4.2 Preparation and Characterization

OEP-Oxime. General procedure for the conversion of 2-Oxochlorin OEP Oxime (14). 2-Oxochlorin **3** (150 mg, 0.27 mmol) was dissolved in (10 mL) pyridine in a 50 mL round-bottom flask equipped with a magnetic stir bar. Solid $NH_2OH \cdot HCl$ (90 eq., 1.69 g) was added to the refluxing reaction mixture. Reaction progress was monitored by TLC and UV-visible spectroscopy. Conversion of the starting material to the product can be identified by the formation of a sharp peak at ~ 653 nm in the UV-visible spectrum of an aliquot of the reaction mixture. The reaction was left stirring until no further reaction was detectable (1 to 2 days). The reaction vessel was then evaporated to dryness by rotary

evaporation. The residue was then dissolved in CH_2Cl_2, and the solution was filtered through a glass frit (M). The volume of the filtrate was reduced, and the mixture was separated by column chromatography (Hexanes/CH_2Cl_2 30-60), to isolate a brownish-purple powder, the oxime **14** (87 mg, 0.15 mmol, 56% yield); starting material **3** was also recovered. MW = 565.8 g/mol; R_f = 0.25 (silica-CH_2Cl_2); UV-visible (CH_2Cl_3) λ_{max} (log ε): 401 (5.29), 502 (4.06), 535 (4.15), 596 (3.68), 654 (4.65) nm; Fluorescence λ_{max} (C_6H_6, λ_{exc} 403 nm): 690, 714, 730 nm ϕ = 0.18; ^{1}H NMR (400 MHz, $CDCl_3$, 25°C): δ = 9.83 (s, 1H), 9.82 (s, 1H), 9.71 (s, 1H), 8.95 (s, 1H), 8.06 (s, 1H), 4.09-3.95 (m, 12H), 3.54-3.44 (m, 2H), 2.84-2.72 (m, 2H), 1.93-1.85 (m, 18H), 0.56 (t, ^3J = 7.4 Hz, 6H), -2.61-2.64 (s, 2H) ppm; ^{13}C NMR (100 MHz; CDCl3): δ = 164.9, 164.7, 150.9, 150.5, 143.2, 143.0, 139.3, 139.2, 137.5, 136.5, 136.3, 135.8, 133.4, 133.2, 98.9, 98.5, 89.5, 89.4, 62.0, 31.7, 19.8, 19.5, 19.44, 19.40, 18.7, 18.6, 18.32, 18.30, 18.2, 18.1, 9.5, 8.5 ppm; HR-MS (ESI+ of $[M + H]^+$, 100% CH_2Cl_2): *m/z* calc'd for $C_{36}H_{47}N_5O$ 566.3859, found 566.3846.

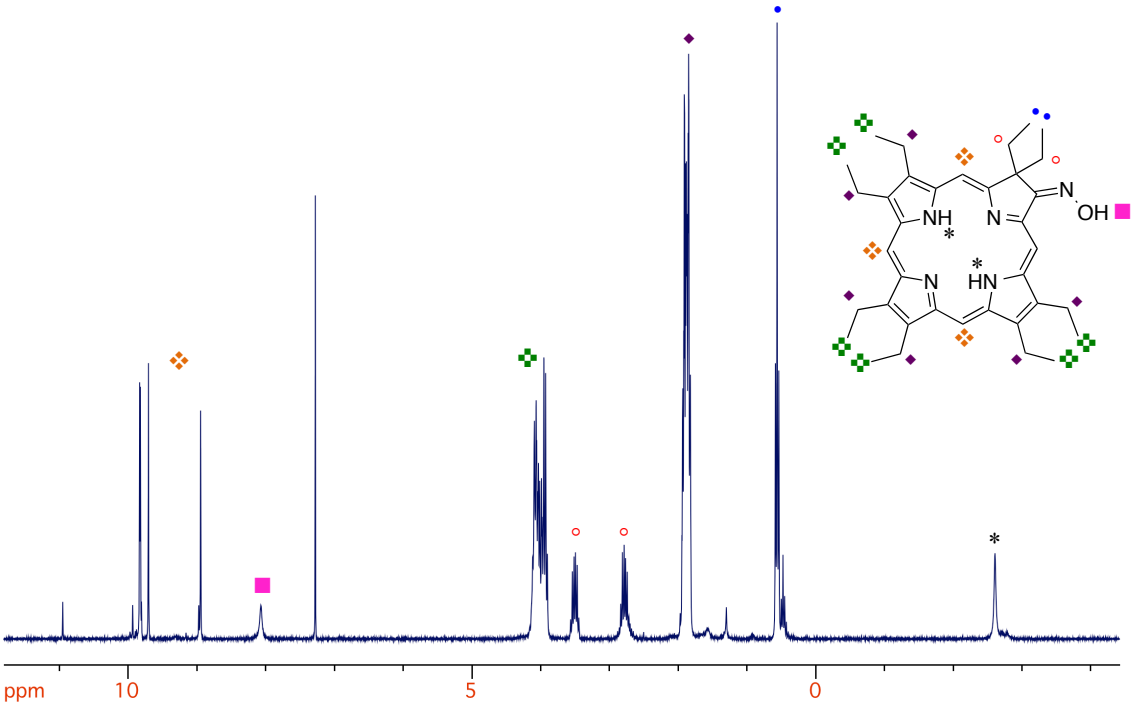

Figure 3-14. ^{1}H NMR spectrum (400 MHz, $CDCl_3$) of **14**.

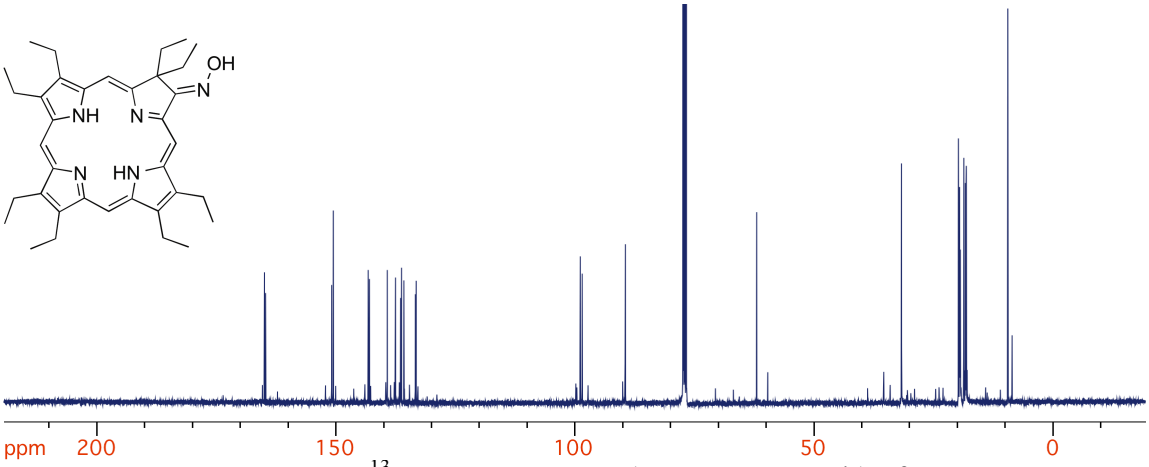

Figure 3-15. ^{13}C NMR spectrum (100 MHz, $CDCl_3$) of **14**.

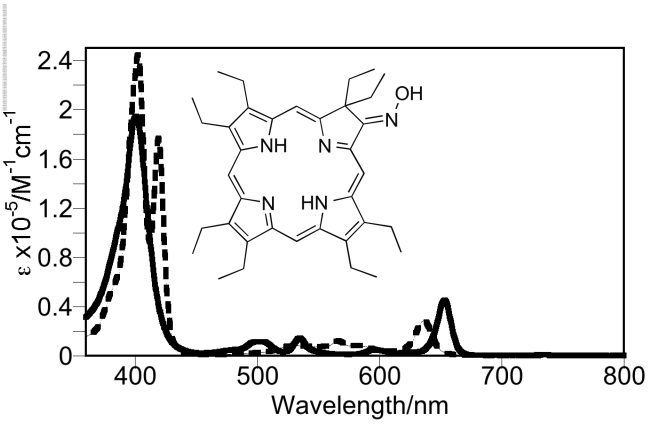

Figure 3-16. UV-vis spectra of **14** in $CHCl_3$ (solid line) and in $CHCl_3$ + 10% TFA (broken line).

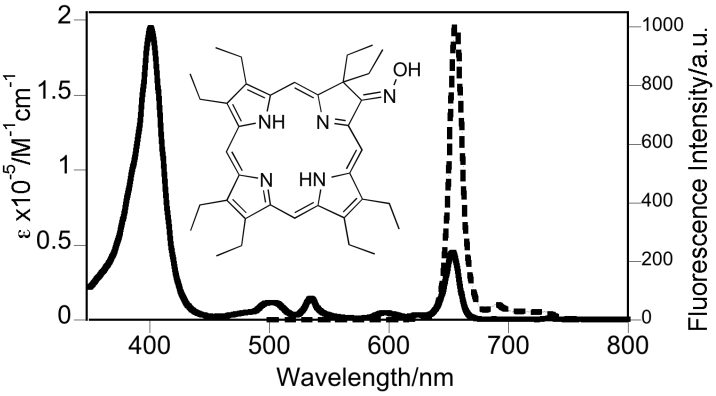

Figure 3-17. UV-vis (solid black trace) ($CHCl_3$) and fluorescence (broken black trace) (C_6H_6) spectra of **14**.

Compound 16: For a typical reaction, a N_2-flushed, 25 mL round bottom flask was loaded with OEP oxime **14** (30 mg, 0.053 mmol) and dissolved in dry THF (2 mL). PCl_5 (30 equiv, 331 mg) dissolved in dry THF was added to the reaction mixture at 0°C, followed by immediate addition of $BF_3{\cdot}OEt_2$ (40 equiv, 0.26 mL). The reaction progress was monitored using TLC and UV-visible spectroscopy. The conversion of starting material to product can be identified by the formation of a peak at ~640 nm with a

neutralized aliquot from the reaction mixture. When the starting material was consumed (~5-10 min), the reaction mixture was quenched using aq NH_4OH (~2.0 mL). After quenching, the reaction mixture was then transferred to a 125 mL separatory funnel, washed with aqueous saturated NaCl and extracted with CH_2Cl_2. The solvents were evaporated to dryness by rotary evaporation and the resulting crude mixture was purified on a preparative TLC plate (Hexanes/CH_2Cl_2 30-60) to furnish an unstable intermediate **16** product as a blue-green powder. The facile susceptibility of this product to air or acid-induced oxidation resulted in the inability to obtain a reliable yield. MW = 565.8 g/mol; R_f = 0.08 (silica-30% hexanes/CH_2Cl_2); UV-visible (CH_2Cl_3) λ_{max} (log ε): 388 (5.02), 494 (3.89), 524 (3.82), 586 (3.52), 640 (4.40) nm; Fluorescence λ_{max} (C_6H_6, λ_{exc} 395 nm): 644 nm, ϕ = 0.05; ^{1}H NMR (400 MHz, $CDCl_3$, 25°C): δ = 9.88 (s, 1H), 9.70 (s, 1H), 9.21 (s, 1H), 8.80 (s, 1H), 4.05-3.95 (m, 12H), 2.94-2.87 (m, ^3J = 14.7, 7.5 Hz, 2H), 2.82-2.75 (m, 3H), 1.89-1.82 (m, ^3J = 12.1, 4.3 Hz, 18H), 1.01 (t, ^3J = 7.3 Hz, 6H), -3.02-3.06 (two br s, 2H) ppm; ^{13}C NMR (100 MHz, CDCl3, 25°C): δ = 206.9, 151.6, 148.8, 147.3, 143.7, 142.2, 139.9, 139.7, 138.5, 137.4, 136.8, 135.4, 134.8, 134.6, 131.4, 100.3, 97.3, 97.0, 87.0, 70.6, 52.7, 36.7, 30.9, 29.7, 19.7, 19.6, 19.50, 19.3, 18.7, 18.5, 18.3, 18.2, 18.0, 17.7, 10.0, 9.6 ppm; HR-MS (ESI+ of $[MH]^+$, 100% CH_2Cl_2): *m/z* calc'd for $C_{36}H_{47}N_5O$ 566.3859, found 566.3889.

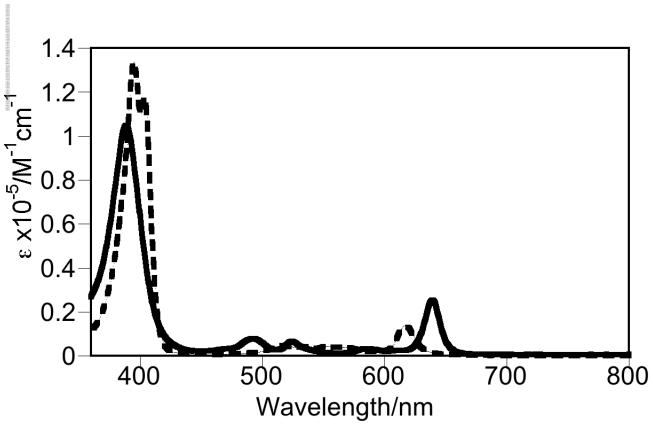

Figure 3-18. UV-vis spectra of compound **16** in $CHCl_3$ (solid line) and in $CHCl_3$ + 10% TFA (broken line).

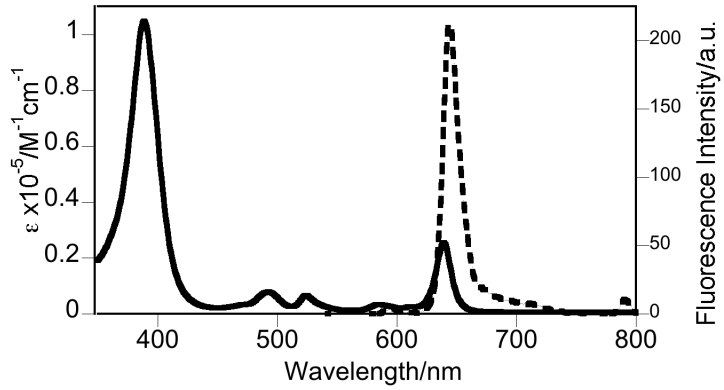

Figure 3-19. UV-vis (solid black trace) ($CHCl_3$) and fluorescence (broken black trace) (C_6H_6) spectra of compound **16**.

OEP-Lactone. General procedure for the conversion of OEP Oxime to 1-Oxa-4-azacyclohexene-based Pyrrole-modified Porphyrin (17): Option A: Prepared as described for the preparation of **16**, **14** (17 mg, 0.03 mmol), PCl_5 (30 equiv, 188 mg) and $BF_3{\cdot}OEt_2$ (40 equiv, 0.15 mL), except exposed to air overnight after chromatographic separation to give **17** (4 mg, 0.007 mmol, 24% yield). Options B: Prepared according to the reaction procedure described for option A, except for the following: After aqueous workup and rotary evaporation to dryness, the crude mixture was redissolved in CH_2Cl_2 and a few drops of TFA added dropwise to the solution, stirred for 5 minutes at ambient temperature. Next, Et_3N was added to the reaction to quench the reaction. The product **17** was isolated by column chromatography (silica-30% hexane/CH_2Cl_2) as a blue powder. MW = 566.8 g/mol; R_f = 0.51 (silica-30%hexanes/CH_2Cl_2); UV-visible (CH_2Cl_3) λ_{max} (log ε): 638 (4.26), 612 (3.20), 584 (3.27), 523 (3.56), 492 (3.74), 388 (4.89) nm; Fluorescence λ_{max} (C_6H_6, λ_{exc} 394 nm): 642 nm, $\phi = 0.09$; ^{1}H NMR (400 MHz, $CDCl_3$, 25°C): δ = 9.94 (s, 1H), 9.78 (s, 1H), 9.20 (s, 1H), 8.96 (s, 1H), 4.11-3.91 (m, 12H), 2.96 (m, ^3J = 14.3, 7.2 Hz, 2H), 2.72 (m, ^3J = 12.8, 6.3 Hz, 2H), 1.91-1.82 (m, 18H), 0.97 (t, ^3J = 7.3 Hz, 6H), -3.20-3.31 (br s, 2H) ppm; ^{13}C NMR (100 MHz, CDCl3, 25°C): δ = 172.9, 167.7, 151.7, 149.5, 146.8, 144.2, 143.9, 142.7, 139.9, 138.9, 137.7, 136.5, 135.8, 134.8, 134.7, 132.5, 131.9, 130.9, 128.8, 100.2, 97.7, 97.4, 87.3, 70.6, 68.2, 56.1, 38.7, 36.2, 30.4, 28.9, 23.8, 23.0, 19.71, 19.68, 19.6, 19.5, 19.3, 18.7, 18.5, 18.3, 18.2, 18.1, 17.8, 14.1, 11.0 ppm; HR-MS (ESI+ of $[MH]^+$, 100% CH_2Cl_2): *m/z* calc'd for $C_{36}H_{46}N_4O_2$ 567.3699, found 567.3672.

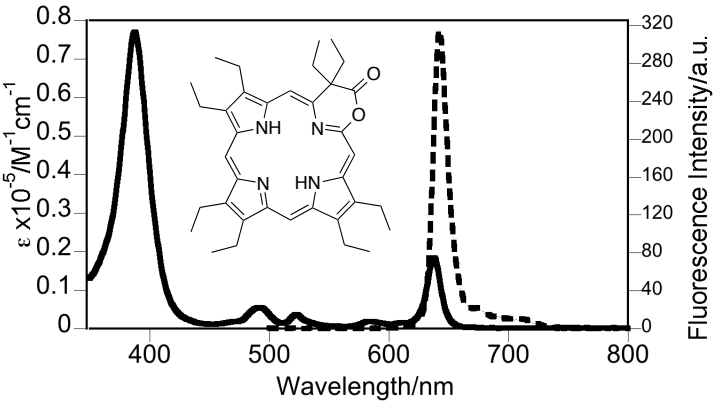

Figure 3-20. UV-vis (solid black trace) ($CHCl_3$) and fluorescence (broken black trace) (C_6H_6) spectra of **17**.

3.5 References

(1) Akhigbe, J.; Ryppa, C.; Zeller, M.; Brückner, C. *J. Org. Chem.* **2009**, *74*, 4927.

(2) Brückner, C.; Dolphin, D. *Tetrahedron Lett.* **1995**, *36*, 3295.

(3) Crossley, M. J.; King, L. G. *J. Chem. Soc., Chem. Commun.* **1984**, 920.

(4) Gouterman, M.; Hall, R. J.; Khalil, G. E.; Martin, P. C.; Shankland, E. G.; Cerny, R. L. *J. Am. Chem. Soc.* **1989**, *111*, 3702.

(5) Khalil, G.; Gouterman, M.; Ching, S.; Costin, C.; Coyle, L.; Gouin, S.; Green, E.; Sadilek, M.; Wan, R.; Yearyean, J.; Zelelow, B. *J. Porphyrins Phthalocyanines* **2002**, *6*, 135.

(6) Köpke, T.; Pink, M.; Zaleski, J. M. *Org. Biomol. Chem.* **2006**, *4*, 4059.

(7) Ogikubo, J., Ph.D. thesis, *University of Connecticut* **2012**.

(8) Zelelow, B. K., G. E.; Phelan, G.; Carlson, B.; Gouterman, M.; Callis, J. B.; Dalton, L. R. *Sens. Actuators, B* **2003**, *96*, 304.

(9) Gouterman, M. C., J.; Dalton, L.; Khalil, G.; Mebarki, Y.; Cooper, K. R.; Grenier, M. Meas. *Sci. Technol.* **2004**, *15*, 1986.

(10) Khalil, G. E. C., C.; Crafton, J.; Jones, G.; Grenoble, S.; Gouterman, M.; Callis, J. B.; Dalton, L. R. *Sens. Actuators, B* **2004**, *97*, 13.

(11) Gouterman, M. *J. Chem. Educ.* **1997**, *74*, 697.

(12) Khalil, G. E. D., P.; Lau, K. S. F.; Imtiaz, S.; King, M.; Gouterman, M.; Sidelev, A.; Puran, N.; Ghandehari, M.; Brückner, C. *Analyst* **2010**, 2125.

(13) Brückner, C.; Ogikubo, J.; McCarthy, J. R.; Akhigbe, J.; Hyland, M. A.; Daddario, P.; Worlinsky, J. L.; Zeller, M.; Engle, J. T.; Ziegler, C. J.; Ranaghan, M. J.; Sandberg, M. N.; Birge, R. R. *J. Org. Chem.* **2012**, *77*, 6480.

(14) McCarthy, J. R. J., H. A.; Brückner, C. *Org. Lett.* **2003**, *5*, 19.

(15) Balasubramanian, T.; Strachan, J.-P.; Boyle, P. D.; Lindsey, J. S. *J. Org. Chem.* **2000**, *65*, 7919.

(16) Strachan, J.-P.; O'Shea, D. F.; Balasubramanian, T.; Lindsey, J. S. *J. Org. Chem.* **2000**, *65*, 3160.

(17) Bonnett, R.; Dolphin, D.; Johnson, A. W.; Oldfield, D.; Stephenson, G. F. *Proc. Chem. Soc.* **1964**, 371.

(18) Chang, C. K. *Biochemistry* **1980**, *19*, 1971.

(19) Inhoffen, H. H.; Nolte, W. *Liebigs Ann. Chem.* **1969**, *725*, 167.

(20) Bonnett, R.; Dimsdale, M. J.; Stephenson, G. F. *J. Chem. Soc. C* **1969**, 564.

(21) Smith, M. B. In *Org. Synth.*; 3rd ed.; 2011, p 188.

(22) Craig, D. In *Comprehensive Organic Synthesis*; Trost, B. M., Fleming, I., Eds.; Pergamon Press: Oxford, 1991; Vol. 7, p 689.

(23) Gawley, R. E. *Org. React. (N.Y.)* **1987**, *35*, 1.

(24) Nguyen, M. T.; Raspoet, G.; Vanquickenborne, L. G. In *Trends in Organic Chemistry*; Aristoff, P. A., Bentrude, W. G., Borden, W. T., Burke, S. D., Curran, D. P., Danheiser, R. L., Danishefsky, S. J., Giese, B., Hanessian, S., Eds.; 1997, *6*, 169.

(25) Torisawa, Y.; Nishi, T.; Minamikawa, J.-i. *Bioorg. Med. Chem. Lett.* **2007**, *17*, 448.

(26) Tandon, V. K.; Awasthi, A. K.; Maurya, H. K.; Mishra, P. *J. Heterocyclic Chem.* **2012**, *49*, 424.

(27) Opanasenko, M.; Shamzhy, M.; Lamač, M.; Čejka, J. *Catalysis Today* **2013**, *204*, 94.

(28) Torisawa, Y.; Nishi, T.; Minamikawa, J.-i. *Bioorg. Med. Chem. Lett.* **2002**, *12*, 387.

(29) Adams, J. P. *Contemp. Org. Synthesis* **1997**, *4*, 517.

(30) Brückner, C.; Akhigbe, J.; Samankumara, L. 'Porphyrin Analogues Containing Non-pyrrolic Heterocycles' in *Handbook of Porphyrin Science*; Eds. Kadish K. M.; Smith, K. M.; Guilard, R.; World Scientific: River Edge, NY. 2014.

(31) Adams, K. R.; Bonnett, R.; Burke, P. J.; Salgado, A.; Vallés, M. A. *J. Chem. Soc. Perkin Trans. 1* **1997**, 1769.

(32) Akhigbe, J.; Brückner, C. *Eur. J. Org. Chem.* **2013**, 3876.

(33) Johnson, A. W.; Oldfield, D. *J. Chem. Soc.* **1965**, 4303.

(34) Stolzenberg, A. M.; Glazer, P. A.; Foxman, B. M. *Inorg. Chem.* **1986**, *25*, 983.

(35) Bagryanskaya, I. Y.; Gatilov, Y. V.; Osadchii, S. A.; Martynov, A. A.; Shakirov, M. M.; Shul'ts, E. E.; Tolstikov, G. A. *Chem. Nat. Compd.* **2005**, *41*, 657.

(36) Mishra, E.; Worlinsky, J. L.; Brückner, C.; Ryzhov, V. *J. Am. Soc. Mass. Spectrom.* **2014**, *25*, 18-29.

(37) Kaczorowska, M. A.; Cooper, H. J. *Chem. Commun.* **2011**, *47*, 418.

(38) Rosario, M.; Domingues, M.; Nemirovskiy, O. V.; Graço O. S. Marques, M.; Graça Neves, M.; Cavaleiro, J. A. S.; Ferrer-Correia, A. J.; Gross, M. L. *J. Am. Mass Spectrom.* **1998**, 767.

(39) Ohno, O.; Kaizu, Y.; Kobayashi, H. *J. Chem. Phys.* **1985**, *82*, 1779.